Available online at www.sciencedirect.com

ScienceDirect

Fuzzy Sets and Systems ••• (••••) •••–•••

FUZZY sets and systems

www.elsevier.com/locate/fss

Recurrent fuzzy wavelet neural network variable impedance control of robotic manipulators with fuzzy gain dynamic surface in an unknown varied environment

Mohammad Hossein Hamedani [a], Maryam Zekri [a,*], Farid Sheikholeslam [a], Mario Selvaggio [b], Fanny Ficuciello [b], Bruno Siciliano [b]

[a] *Department of Electrical and Computer Engineering, Isfahan University of Technology, Isfahan 84156-83111, Iran*
[b] *Department of Electrical Engineering and Information Technology, University of Naples Federico II, Naples, Italy*

Received 21 October 2019; received in revised form 5 March 2020; accepted 6 May 2020

Abstract

In this paper, an intelligent variable impedance control combined with a fuzzy gain dynamic surface is proposed to improve the interaction of the robot manipulator with an unknown varied environment. The parameters of the proposed variable impedance are adapted by optimization an introduced cost function using a recurrent fuzzy wavelet network. The stability conditions for the varying inertial, stiffness and damping are presented to guarantee the stability of the variable impedance. Additionally, a fuzzy dynamic surface method is developed to tune the gains of the dynamic surface as a robust controller. The proposed fuzzy gain dynamic surface is used to force the end-effector of the manipulator to track the desired impedance profile in the presence of large disturbances. Using Lyapunov's method, the stability of the mentioned closed-loop system is proved. Finally, by using a designed simulator for IRB120 (ABB) robot, several simulations are carried out to verify the performance of the proposed method for the execution of various tasks in an unknown varied environment in the presence of large disturbances.

Keywords: Intelligent impedance control; Robotic manipulator; Recurrent fuzzy wavelet neural networks; Fuzzy dynamic surface control

1. Introduction

Impedance control is a classical control method to realize compliant behavior in the robotic manipulators. Hogan in [1] introduced the main concept of the impedance controller that nowadays is considered a main compliant controller. The main statement of the impedance control is that the end-effector should modulate its behavior according to interaction with the environment. When a robot interacts with an unknown varied environment, the impedance

* Corresponding author.
E-mail address: mzekri@iut.ac.ir (M. Zekri).

https://doi.org/10.1016/j.fss.2020.05.001
0165-0114/

Please cite this article in press as: M.H. Hamedani et al., Recurrent fuzzy wavelet neural network variable impedance control of robotic manipulators with fuzzy gain dynamic surface in an unknown varied environment, Fuzzy Sets Syst. (2020), https://doi.org/10.1016/j.fss.2020.05.001

parameters are necessary to be tuned in order to perform various tasks. In fact, the variable impedance control gives the robustness and the flexibility to change impedance and dynamic interaction of the end-effector in a continuous manner during task execution. In the following introduction section, we considered two procedures. First, we study the variable impedance control and its challenges. Additionally, we present the intelligent variable impedance method as one of the main continuations of our research. Then, we study the dynamic surface as a nonlinear controller used to force the robot manipulator to track the variable impedance profile. To present a robust controller in this work, we propose the fuzzy gain dynamic surface to observe and eliminate the uncertainties and disturbances.

There are several works that have addressed the variable impedance methods. In [2–4], variable impedance control is accomplished by using reinforcement learning methods. In [5], a novel design and fabrication methodologies are addressed to produce cost effective hardware prototypes for investigating the efficacy of the variable impedance approach. In [6], an adaptive impedance control approach is proposed to adjust the stiffness on-line using the tracking error of the motion trajectory. In [7], a fuzzy approach is used to generate the impedance gain to guarantee a certain contact force on the contour of the fixed environment. In [8], the impedance parameters are modulated on-line according to human behavior during the interaction. In [9], an iterative learning control method is proposed for impedance control robotics tasks when the endpoint of soft tool interacts with a rigid object or environment at a certain periodic force pattern. Seraji et al. [10] have used the direct and indirect adaptive method to generate the reference position and the estimated parameters of the unknown environment.

However, only a limited number of the works have addressed the stability conditions for the variable impedance profile. In fact, the impedance control with constant gains ensures the stability of the closed-loop system, and it makes a stable behavior of the system both in free motion and in case of interaction with passive environments [11,12]. However, stability is lost if the impedance parameters are considered time varying. The authors in [13] have analyzed the stability conditions for varying stiffness and damping. In [14], a switched stiffness approach is presented for vibration control. Ferraguti et al. [15] presented the tank-based approach to guarantee the system passivity for time varying stiffness. Selvaggio et al. [16] proposed an online technique to adapt the pose and geometry of virtual fixtures and used the tank-theory to guarantee the stability of the systems. In [17], a multi-layer perceptron network was used to estimate and regulate the impedance parameters without considering the stability of the impedance profile. Therefore, we have to present a stability condition for the variable impedance control.

In this work, an adaptive control method is proposed to optimize a cost function using Recurrent Fuzzy Wavelet Neural Network (RFWNN). In fact, the presented method is an online learning approach to tune the impedance parameters of the robot manipulator. According to the task requirements such as convergence to the desired environment without large overshooting or with an acceptable desired force tracking, the cost function is defined to improve the interaction of the robot manipulator. It is worth to mention that, RFWNNs have both the properties of the fuzzy logic and wavelet neural networks. In fact, the combination of the fuzzy mechanism as an effective solution for dealing with a complex nonlinear process and wavelet neural network as an approach for estimation of the local changes makes a powerful adaptive method to model the nonlinear dynamics [18–20]. Additionally, the recurrent property of the RFWNN is able to store the past information of the network and use it to estimate the model of sudden jumps of the dynamical system. In addition, a stabilizer coefficient is proposed to guarantee the stability of the variable impedance. Therefore, the presented approach leads to improve the stability and robustness of the variable impedance profile while the robot interacts with a varied and unknown environment.

Because of the nonlinear dynamics of the robot manipulators, it is necessary to use an effective nonlinear control such as sliding mode control [21], feedback linearization [22] or the backstepping control [23,24] to force the robot manipulator to track the generated impedance profile. In [25], an event-triggered control method is developed using backstepping approach and according to a nonlinear decomposition of input quantization. Additionally, Two methods can be considered including force impedance control or position-based impedance control [26,27]. In our work, we present a fuzzy approach to tune the gains of the dynamic surface as a robust force impedance control.

There are several works addressed disturbances and saturation problems in the control systems [28–31]. In [32], an interval type-2 fuzzy approach is used to detect the fault in the sensor saturation for continues-time fuzzy semi-Markov jump [33] systems. With respect to the previous works, the presented fuzzy approach, as a simple structure, is able to remove the external disturbances to handle saturation and to improve the response of the actuators. Furthermore, the dynamic surface control technique can solve the problem of the "explosion of complexity" caused by repeated differentiation of virtual controllers during the recursive procedures in the back-stepping method [34,35]. The dynamic surface solves this problem by using a low-pass filter of the synthetic virtual control law at each step of

Please cite this article in press as: M.H. Hamedani et al., Recurrent fuzzy wavelet neural network variable impedance control of robotic manipulators with fuzzy gain dynamic surface in an unknown varied environment, Fuzzy Sets Syst. (2020), https://doi.org/10.1016/j.fss.2020.05.001

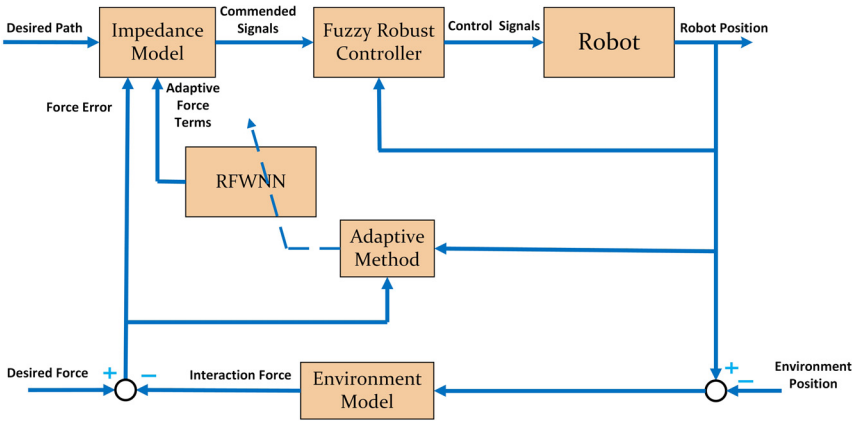

Fig. 1. The block diagram illustrates the closed loop system. The inner loop (includes FGDS, Robot and robot state feedback) and the outer loop (includes variable impedance, FGDS, Robot and robot state feedback).

the back-stepping procedure [34]. Several works have addressed the dynamic surface control using adaptive methods in the robotic systems [36–39]. However, in our work, the gains of the dynamic surface are adapted with respect to the presence of uncertainty and disturbances using the fuzzy approach. Therefore, the simple presented method leads to improve the robustness of the robot manipulators. Additionally, we used the dynamic surface methods as a novel application of this approach to obtain a simple structure, the target impedance is formulated in the state space, and effective dynamic surfaces are defined to track the desired impedance behavior. In fact, dynamic surface control is used to force the robot manipulator to track the desired impedance, while the robot interacts with an environment.

According to the above discussion, this paper presents an intelligent and robust impedance control of the robot manipulators to interact with the unknown varied environment. According to Fig. 1, the proposed controller includes two closed loops. The outer loop is related to the intelligent variable impedance and the inner loop is considered for the fuzzy gain dynamic surface. Using the Lyapunov method, the stability conditions are induced to guarantee the bounded signals in the closed-loop system. The contributions of this paper are summarized as follows:

- An adaptive control method is proposed to optimize a cost function based on the recurrent fuzzy wavelet neural network as an online learning approach to tune the impedance parameters of the robot manipulator. In the proposed approach the impedance parameters including inertial, damping and stiffens are considered as only one parameter and are estimated by the RFWNN. It leads to decrease the computational complexity. Additionally, the introduced online learning approach improves the interaction of the robot with the environment and effectively reduces the contact force error with an acceptable transient response.
- To solve the large external disturbances, we have designed an effective impedance controller based on the Fuzzy Gain Dynamic Surface (FGDS). As a novel application of the dynamic surface method to obtain a simple structure, which the target impedance is formulated in the state space, and effective dynamic surfaces are defined to track the desired impedance behavior. Additionally, FGDS is able to estimate the unknown uncertainties and disturbances of the robotic system. In fact, introduced dynamic surface control in combination with the fuzzy rules is able to force the end-effector of the robot manipulator to track the desired impedance model.

The rest of this paper is organized as follows: In section 2, the system dynamics of the robot manipulators and the variable impedance are presented. Section 3 proposes the intelligent variable impedance control and fuzzy gain dynamic surface. Additionally, the stability conditions are analyzed by Lyapunov stability theory. Section 4 shows the performance of the proposed approach using the designed simulator for the IRB120 ABB robot, and the last section concludes with a short summary of the paper.

Please cite this article in press as: M.H. Hamedani et al., Recurrent fuzzy wavelet neural network variable impedance control of robotic manipulators with fuzzy gain dynamic surface in an unknown varied environment, Fuzzy Sets Syst. (2020), https://doi.org/10.1016/j.fss.2020.05.001

2. Preliminaries and problem formulation

Nominal and actual rigid-body dynamic of the robot manipulator are described in Section 2.1. In order to use the dynamic surface as a nonlinear approach, the actual dynamic of the manipulator is formulated in the state space. Additionally, the variable target impedance is defined in Section 2.2.

2.1. Rigid body dynamics

A rigid-body form describing the nominal dynamic equations of the n-link robot manipulator accurately can be considered as follows:

$$\boldsymbol{H}(\boldsymbol{q})\ddot{\boldsymbol{q}} + \boldsymbol{V}(\boldsymbol{q},\dot{\boldsymbol{q}}) + \boldsymbol{G}(\boldsymbol{q}) + \boldsymbol{J}^T(\boldsymbol{q})\mathbf{f_e} + \tilde{\boldsymbol{f}} = \boldsymbol{\tau}\,, \tag{1}$$

where $\boldsymbol{q} \in \mathbb{R}^{n\times 1}$ is the joint displacement vector, $\boldsymbol{\tau} \in \mathbb{R}^{n\times 1}$ refers to the applied joint torque or force signal control, $\boldsymbol{H}(\boldsymbol{q}) \in \mathbb{R}^{n\times n}$ denotes the inertia matrix, $\boldsymbol{V}(\boldsymbol{q},\dot{\boldsymbol{q}}) \in \mathbb{R}^{n\times 1}$ shows the Coriolis and centrifugal vector, $\boldsymbol{G}(\boldsymbol{q}) \in \mathbb{R}^{n\times 1}$ illustrates the gravitational vector and $\boldsymbol{J}(\boldsymbol{q})$ stands for the Jacobin matrix. $\mathbf{f_e}$ is the interaction forces vector and $\tilde{\boldsymbol{f}}$, as the external disturbances and described in the joint space, introduces uncertainty of the interaction forces. Assuming that the system states $\boldsymbol{q}, \dot{\boldsymbol{q}}$ and interaction force $\mathbf{f_e}$ are available for feedback.

Because of model uncertainty and external disturbance, the nominal values of $\boldsymbol{H}(\boldsymbol{q})$, $\boldsymbol{V}(\boldsymbol{q},\dot{\boldsymbol{q}})$ and $\boldsymbol{G}(\boldsymbol{q})$ are different from the actual values $\hat{\boldsymbol{H}}(\boldsymbol{q})$, $\hat{\boldsymbol{V}}(\boldsymbol{q},\dot{\boldsymbol{q}})$ and $\hat{\boldsymbol{G}}(\boldsymbol{q})$, respectively. Consequently, the nominal values are known and the actual values and $\tilde{\boldsymbol{f}}$, as the external disturbances, are unknown.

Assumption 1. Modeling errors values are bounded although they are not available. The bounds of the modeling errors are assumed as follows:

$$|\Delta\boldsymbol{H}(\boldsymbol{q})| \le \delta \qquad \Delta\boldsymbol{H}(\boldsymbol{q}) = \boldsymbol{H}(\boldsymbol{q}) - \hat{\boldsymbol{H}}(\boldsymbol{q})\,, \tag{2a}$$

$$|\Delta\boldsymbol{V}(\boldsymbol{q},\dot{\boldsymbol{q}})| \le \delta \qquad \Delta\boldsymbol{V}(\boldsymbol{q},\dot{\boldsymbol{q}}) = \boldsymbol{V}(\boldsymbol{q},\dot{\boldsymbol{q}}) - \hat{\boldsymbol{V}}(\boldsymbol{q},\dot{\boldsymbol{q}})\,, \tag{2b}$$

$$|\Delta\boldsymbol{G}(\boldsymbol{q})| \le \delta \qquad \Delta\boldsymbol{G}(\boldsymbol{q}) = \boldsymbol{G}(\boldsymbol{q}) - \hat{\boldsymbol{G}}(\boldsymbol{q})\,, \tag{2c}$$

$$|\Delta\tilde{\boldsymbol{f}}| \le \delta\,. \tag{2d}$$

The actual dynamics of the n-link robot system (1) is expressed as:

$$\hat{\boldsymbol{H}}(\boldsymbol{q})\ddot{\boldsymbol{q}} + \hat{\boldsymbol{V}}(\boldsymbol{q},\dot{\boldsymbol{q}}) + \hat{\boldsymbol{G}}(\boldsymbol{q}) + \boldsymbol{J}^T(\boldsymbol{q})\mathbf{f_e} + \tilde{\boldsymbol{f}} = \boldsymbol{\tau}\,. \tag{3}$$

Using nominal model (1) and actual robot dynamic (3), we have

$$\boldsymbol{H}(\boldsymbol{q})\ddot{\boldsymbol{q}} + \boldsymbol{V}(\boldsymbol{q},\dot{\boldsymbol{q}}) + \boldsymbol{G}(\boldsymbol{q}) + \boldsymbol{J}^T(\boldsymbol{q})\mathbf{f_e} + \Pi = \boldsymbol{\tau}\,, \tag{4}$$

where $\boldsymbol{\Pi}$ denotes the uncertainty of robot dynamics and disturbance effects defined as follows:

$$\begin{aligned}\boldsymbol{\Pi} = &-\boldsymbol{H}(\boldsymbol{q})\hat{\boldsymbol{H}}(\boldsymbol{q})^{-1}\{-\tilde{\boldsymbol{f}} - \hat{\boldsymbol{V}}(\boldsymbol{q},\dot{\boldsymbol{q}}) - \hat{\boldsymbol{G}}(\boldsymbol{q}) - \boldsymbol{J}^T(\boldsymbol{q})\mathbf{f_e} + \boldsymbol{\tau}\}\\ &+\{-\boldsymbol{V}(\boldsymbol{q},\dot{\boldsymbol{q}}) - \boldsymbol{G}(\boldsymbol{q}) - \boldsymbol{J}^T(\boldsymbol{q})\mathbf{f_e} + \boldsymbol{\tau}\}\,.\end{aligned} \tag{5}$$

$\boldsymbol{x}_{R_1} = \boldsymbol{q}$, $\boldsymbol{x}_{R_2} = \dot{\boldsymbol{q}}$ are defined as the state space variables, and the robot dynamic system with uncertainty terms (5) can be described as follows:

$$\dot{\boldsymbol{x}}_{R_1} = \boldsymbol{x}_{R_2}\,, \tag{6}$$

$$\dot{\boldsymbol{x}}_{R_2} = \boldsymbol{H}(\boldsymbol{x}_{R_1})^{-1}\{-\boldsymbol{V}(\boldsymbol{x}_{R_1},\boldsymbol{x}_{R_2}) - \boldsymbol{G}(\boldsymbol{x}_{R_1}) - \boldsymbol{J}^T(\boldsymbol{x}_{R_1})\mathbf{f_e} + \boldsymbol{\tau}\} + \mathbf{U}\,, \tag{7}$$

where

$$\boldsymbol{U} = -\boldsymbol{H}(\boldsymbol{x}_{R_1})^{-1}\boldsymbol{\Pi} \tag{8}$$

is considered as unknown dynamic uncertainty and disturbance effects.

Please cite this article in press as: M.H. Hamedani et al., Recurrent fuzzy wavelet neural network variable impedance control of robotic manipulators with fuzzy gain dynamic surface in an unknown varied environment, Fuzzy Sets Syst. (2020), https://doi.org/10.1016/j.fss.2020.05.001

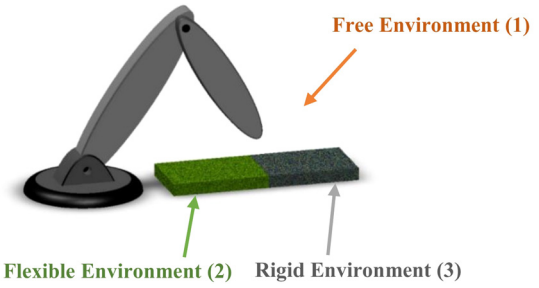

Fig. 2. Maneuver of the robot manipulator in the varied environments.

2.2. General variable impedance

The desired impedance is specified as:

$$\boldsymbol{M}_d\ddot{\tilde{\boldsymbol{x}}} + \boldsymbol{B}_d\dot{\tilde{\boldsymbol{x}}} + \boldsymbol{K}_d\tilde{\boldsymbol{x}} = -\boldsymbol{e}_f\,, \tag{9}$$

where $\tilde{\boldsymbol{x}} = \boldsymbol{x}_I(t) - \boldsymbol{x}_d(t)$ and $\boldsymbol{e}_f = \boldsymbol{f}_d(t) - \boldsymbol{f}_e(t)$. $\boldsymbol{x}_d(t) \in \mathbb{R}^{m\times 1}$ is a smooth desired trajectory in the task space and $\boldsymbol{x}_I(t) \in \mathbb{R}^{m\times 1}$ is the reference trajectory realized by the impedance profile. The dimension of the task space is denoted by m. $\boldsymbol{f}_d$ and $\boldsymbol{f}_e \in \mathbb{R}^{m\times 1}$ are the environment and desired force, respectively. $\boldsymbol{M}_d(t)$, $\boldsymbol{B}_d(t)$, and $\boldsymbol{K}_d(t)$ are $m \times m$ time varying desired inertia, damping, and stiffness, receptively. Frequently, the impedance parameters are selected as diagonal matrices to obtain linear and decoupled response.

The objective of the control is to design a control approach so that the impedance of the robot manipulator tracks the given variable target impedance (9) under assuming uncertainties and disturbances modeling (8). To that end, we define $z_1 = \boldsymbol{x}_I$ and $z_1 = \dot{\boldsymbol{x}}_I$ as the state variables of the desired impedance (9) described as follows:

$$\dot{z}_1 = z_2\,, \tag{10}$$

$$\dot{z}_2 = \ddot{\boldsymbol{x}}_d(t) - \boldsymbol{M}_d(t)^{-1}\{\boldsymbol{e}_f + \boldsymbol{B}_d\dot{\tilde{\boldsymbol{x}}} + \boldsymbol{K}_d\tilde{\boldsymbol{x}}\}\,. \tag{11}$$

In this work, we consider varying impedance control using an intelligent approach, which gives the flexibility to change impedance and dynamic interaction of the manipulator end-effector in a continuous manner during the task. According to Fig. 2, the following three scenarios can be considered for the robot manipulator motion:

- **Environment (1):** robot moves in the free space where $\boldsymbol{f}_e = 0$.
- **Environment (2):** robot interacts with flexible environment so that $\boldsymbol{f}_e \neq 0$ and $\boldsymbol{f}_e$ is small.
- **Environment (3):** robot interacts with the rigid environment so that $\boldsymbol{f}_e \neq 0$ and $\boldsymbol{f}_e$ is big.

In all defined scenarios, the end-effector response is to comply with the contact forces defined by target impedance (9).

One of the challenges is tuning the parameters of impedance (9) according to varied and unknown environment in order to improve the interaction between the robot and the environment. Additionally, the controller needs to be robust to remove uncertainty and disturbance term (8).

3. Proposed controller

To present a proper controller to handle the disturbances and generate an impedance profile according to a varied environment, a novel stable controller consisting of the RFWNN impedance and a fuzzy gain dynamic surface is proposed. The RFWNN variable impedance is presented as a method to interact with an unknown varied environment. Furthermore, the proposed fuzzy gain dynamic surface is formulated to remove the disturbances and to make a tradeoff between the robustness and accuracy to track the desired impedance profile. Finally, the stability of the proposed controller is proved using Lyapunov's method.

Please cite this article in press as: M.H. Hamedani et al., Recurrent fuzzy wavelet neural network variable impedance control of robotic manipulators with fuzzy gain dynamic surface in an unknown varied environment, Fuzzy Sets Syst. (2020), https://doi.org/10.1016/j.fss.2020.05.001

3.1. Proposed variable impedance control

As mentioned in Section 2.2, there are three scenarios when the robot interacts with the unknown varied environment. To have an acceptable interaction, the robot needs to adapt the impedance parameters. Therefore, the impedance profile can be proposed as follows:

$$(\boldsymbol{M}_{dc} + \boldsymbol{M}_{dv}(t))\ddot{\tilde{\boldsymbol{x}}} + (\boldsymbol{B}_{dc} + \boldsymbol{B}_{dv}(t))\dot{\tilde{\boldsymbol{x}}} + (\boldsymbol{K}_{dc} + \boldsymbol{K}_{dv}(t))\tilde{\boldsymbol{x}} = -\boldsymbol{e}_f\,. \tag{12}$$

In (12), each of the desired impedance parameters has two parts including constant parameters such as $\boldsymbol{M}_{dc}$, $\boldsymbol{B}_{dc}$, and $\boldsymbol{K}_{dc}$ and variable parts $\boldsymbol{M}_{dv}(t)$, $\boldsymbol{B}_{dv}(t)$, and $\boldsymbol{K}_{dv}(t)$. Now, (12) is rewritten as follows:

$$\boldsymbol{M}_{dc}\ddot{\tilde{\boldsymbol{x}}} + \boldsymbol{B}_{dc}\dot{\tilde{\boldsymbol{x}}} + \boldsymbol{K}_{dc}\tilde{\boldsymbol{x}} = -\boldsymbol{e}_f - \boldsymbol{M}_{dv}(t)\ddot{\tilde{\boldsymbol{x}}} - \boldsymbol{B}_{dv}(t)\dot{\tilde{\boldsymbol{x}}} - \boldsymbol{K}_{dv}(t)\tilde{\boldsymbol{x}}\,, \tag{13}$$

$$\ddot{\tilde{\boldsymbol{x}}} + \boldsymbol{M}_{dc}{}^{-1}\boldsymbol{B}_{dc}\dot{\tilde{\boldsymbol{x}}} + \boldsymbol{M}_{dc}{}^{-1}\boldsymbol{K}_{dc}\tilde{\boldsymbol{x}} = -\boldsymbol{M}_{dc}{}^{-1}\boldsymbol{e}_f - \boldsymbol{M}_{dc}{}^{-1}\boldsymbol{K}_s(t)\boldsymbol{f}_o(\tilde{\boldsymbol{x}}, \dot{\tilde{\boldsymbol{x}}}, \ddot{\tilde{\boldsymbol{x}}})\,, \tag{14}$$

$$\ddot{\boldsymbol{x}}_i = \ddot{\boldsymbol{x}}_d - \boldsymbol{M}_{dc}{}^{-1}[\boldsymbol{B}_{dc}\dot{\tilde{\boldsymbol{x}}} + \boldsymbol{K}_{dc}\tilde{\boldsymbol{x}} + \boldsymbol{e}_f] - \boldsymbol{M}_{dc}{}^{-1}\boldsymbol{K}_s(t)\boldsymbol{f}_o(\tilde{\boldsymbol{x}}, \dot{\tilde{\boldsymbol{x}}}, \ddot{\tilde{\boldsymbol{x}}})\,, \tag{15}$$

where $\ddot{\boldsymbol{x}}_i$ is the proposed acceleration by the variable impedance profile. Additionally, the variable parameter parts of (13) are substituted by the $\boldsymbol{K}_s(t)\boldsymbol{f}_o$ term, where $\boldsymbol{K}_s(t)$ is a stabilizer coefficient and is defined as:

$$\boldsymbol{K}_s(t) = \begin{cases} k_s & \dot{\tilde{\boldsymbol{x}}}\boldsymbol{f}_o \geq 0 \\ k_s & \dot{\tilde{\boldsymbol{x}}}\boldsymbol{f}_o < 0 \text{ and } |\dot{\tilde{\boldsymbol{x}}}^T k_s \boldsymbol{f}_o| < \dot{\tilde{\boldsymbol{x}}}^T \boldsymbol{B}_{dc}\dot{\tilde{\boldsymbol{x}}} \\ 0 & \dot{\tilde{\boldsymbol{x}}}\boldsymbol{f}_o < 0 \text{ and } |\dot{\tilde{\boldsymbol{x}}}^T k_s \boldsymbol{f}_o| \geq \dot{\tilde{\boldsymbol{x}}}^T \boldsymbol{B}_{dc}\dot{\tilde{\boldsymbol{x}}}\,, \end{cases} \tag{16}$$

where $k_s > 0$ shows a constant and design parameter. In fact, $\boldsymbol{K}_s(t)$ is used to guarantee the stability of the variable impedance profile both in free motion and in case of interaction with varied environments. The condition for $\boldsymbol{K}_s(t)$ is explained more in detail in the proof of Theorem 1. In addition, $\boldsymbol{f}_o$ is the variable impedance part of (13) and is adapted by the RFWNN. By adapting $\boldsymbol{f}_o$, the robot is able to interact with the varied and unknown environments. The main advantage of the proposed variable impedance (15) is that the robot just needs to adapt $\boldsymbol{f}_o$ instead of adapting $\boldsymbol{M}_{dv}(t)$, $\boldsymbol{B}_{dv}(t)$, and $\boldsymbol{K}_{dv}(t)$ in order to interact with the environment. In addition, the stability of the time-varying impedance profile is guaranteed using the $\boldsymbol{K}_s(t)$ term.

3.2. RFWNN

Since the robot manipulators operate in different workspaces, the properties of the environment such as stiffness or damping are variously unknown. Thus, offline learning methods are not served and online learning approaches with fast convergence should necessarily be applied. Hence, RFWNN is considered an adaptive network to estimate $\boldsymbol{f}_o$ in (15) by observing the behavior of the robot and properties of the environment.

In this study, the structure of the RFWNN model is presented in Fig. 3. RFWNN integrates the Takagi-Sugeno-Kang (TSK) fuzzy model with the recurrent wavelet neural networks. The kernel of the fuzzy model is the fuzzy knowledge and the consequent part of the TSK fuzzy rules are constant or a function. Fuzzy models cannot be applied to approximate local dynamics. In general, they are not able to estimate the local time-frequency of nonlinear system sudden changes or discontinuity [40] because of their structures. In addition, their convergence is not generally fast. However, the wavelet transform provides a time-frequency localization of the approximated signal. WNNs have properties such as the high resolution of wavelets, which can be used to estimate local changes [41–45], learning capability and global approximation of NNs. On the other hand, the WNNs have feed-forward structures and are able to estimate a static model. To estimate and represent dynamic mapping, the self-recurrent wavelet neural network (SRWNN), which has the properties of recurrent neural networks (RNNs) [46,47] and local approximation of WNNs, has been proposed to control a flexible-joint robot [36]. SRWNNs have a mother-wavelet layer composed of self-feedback neurons. Actually, they can store the past information of the network to model sudden jumps of the environment. Because of the above-mentioned reasons, in this paper, RFWNNs are used to model and estimate the variable part of the impedance profile. The rules used in the RFWNN have the following structures (Table 1), where $\boldsymbol{R} = \{\mathbf{R_1}, \mathbf{R_2}, ..., \mathbf{R_n}\}$ are the rules, $\boldsymbol{x} = \{\mathbf{x_1}, \mathbf{x_2}, ..., \mathbf{x_m}\}$ are the input variables, and A_{nm} is the mth Gaussian type membership function for nth rule. The Mexican Hat as i.e. $\varphi(z) = (1 - z^2)e^{-\frac{1}{2}z^2}$ is used as mother-wavelet function for the conclusion parts of

Please cite this article in press as: M.H. Hamedani et al., Recurrent fuzzy wavelet neural network variable impedance control of robotic manipulators with fuzzy gain dynamic surface in an unknown varied environment, Fuzzy Sets Syst. (2020), https://doi.org/10.1016/j.fss.2020.05.001

Table 1
Fuzzy rules for recurrent wavelet neural network.

Rule No.	IF	THEN
$\mathbf{R_1}$	$\boldsymbol{x}_1$ is A_{11} and $\boldsymbol{x}_2$ is A_{12} and ... and $\boldsymbol{x}_m$ is A_{1m}	$y_1 = \sum_{i=1}^{m} \boldsymbol{w}_{i1}(1 - z_{11}^2)e^{-z_{11}^2/2}$
$\mathbf{R_2}$	$\boldsymbol{x}_1$ is A_{21} and $\boldsymbol{x}_2$ is A_{22} and ... and $\boldsymbol{x}_m$ is A_{2m}	$y_2 = \sum_{i=1}^{m} \boldsymbol{w}_{i2}(1 - z_{21}^2)e^{-z_{21}^2/2}$
...	...	...
$\mathbf{R_n}$	$\boldsymbol{x}_1$ is A_{n1} and $\boldsymbol{x}_2$ is A_{n2} and ... and $\boldsymbol{x}_m$ is A_{nm}	$y_n = \sum_{i=1}^{m} \boldsymbol{w}_{in}(1 - z_{n1}^2)e^{-z_{n1}^2/2}$

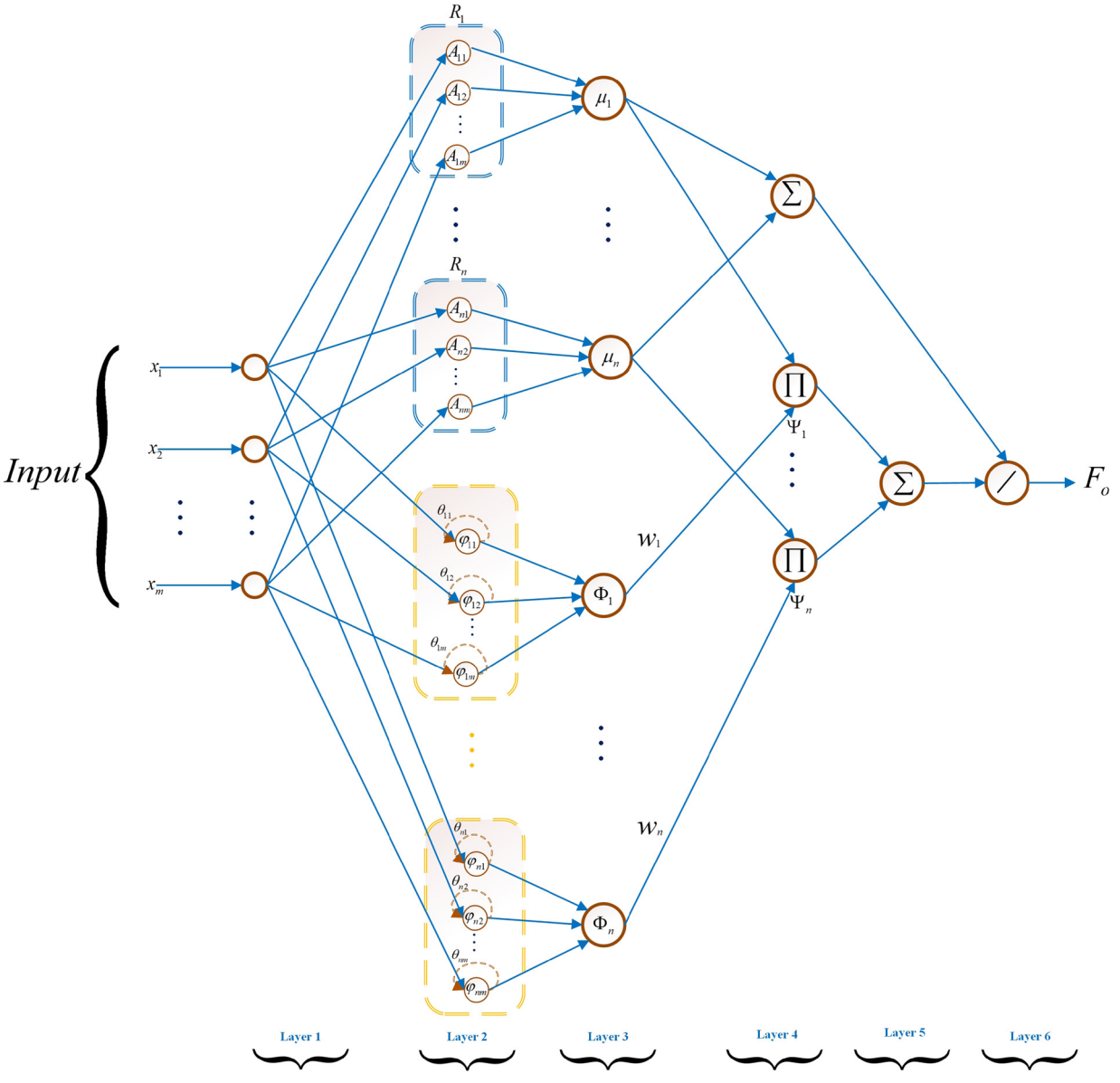

Fig. 3. The structure of the RFWNN.

Please cite this article in press as: M.H. Hamedani et al., Recurrent fuzzy wavelet neural network variable impedance control of robotic manipulators with fuzzy gain dynamic surface in an unknown varied environment, Fuzzy Sets Syst. (2020), https://doi.org/10.1016/j.fss.2020.05.001

the TKS fuzzy rules. The structure of the RFWNN is depicted in Fig. 3, and it has six layers with dynamic feedback connection.

In the first layer, each node is an input node corresponding to one input variable. These nodes are used to distinguish each of the input signals. In the second layer, the If part of the fuzzy rules and wavelones are implemented. For the fuzzy sections of Layer 2, the membership degree is calculated for each entering input signals from Layer 1. The Gaussian functions are considered membership functions as follows:

$$\boldsymbol{A}_{ji}(x_i) = e^{\frac{-(x_i - c_{ji})^2}{\sigma_{ji}^2}}, \qquad i = 1, ..., m, \qquad j = 1, ..., n, \tag{17}$$

where m is the number of input signals, n refers to the number of the fuzzy rules, $\boldsymbol{A}_{ji}(x_i)$ shows the jth membership function for the ith input variable, and c_{ji} and σ_{ji} represent the center and width of the Gaussian membership function, respectively. In addition, each wavelone of Layer 2 can be obtained as:

$$\Phi_j = \prod_{i=1}^{m} \varphi_{ji}(z_{ji}), \quad z_{ji} = \frac{u_{ji} - b_{ji}}{a_{ji}}, \quad i = 1, ..., m, \qquad j = 1, ..., n, \tag{18}$$

where b_{ji} and a_{ji} are the translation, and the dilation factors of the mother-wavelet, respectively. In addition, the inputs of the wavelet nodes u_{ji} are defined as:

$$u_{ji} = x_i + \varphi_{ji}^{\text{old}}\theta_{ji}, \qquad i = 1, ..., m, \qquad j = 1, ..., n, \tag{19}$$

where θ_{ji} represents the information storage parameters, and $\varphi_{ji}^{\text{old}}$ is the previous value of mother-wavelet function of network. The main aspect of RFWWN is the feedback term, which stores the past information and current dynamics of the network for the next sample.

In the third layer, the number of nodes is equal to that of rules $\mathbf{R_1}, \mathbf{R_2}, ..., \mathbf{R_n}$ and wavelones. In fact, each node corresponds to one fuzzy rule and one wavelone. In this paper, the AND(product) operation is used to calculate $\mu_1, \mu_2, ..., \mu_n$ as:

$$\mu_j = \prod_{i=1}^{m} \boldsymbol{A}_{ji}(x_i), \qquad i = 1, ..., m, \qquad j = 1, ..., n. \tag{20}$$

The μ_j are considered as input signals for the consequent layer. The output of the lth wavelet layer is

$$\Psi j = w_j \Phi_j, \qquad j = 1, ..., n. \tag{21}$$

In the fourth layer, we have

$$\boldsymbol{y} = \sum_{j=1}^{n} \mu_j \Psi j, \qquad j = 1, ..., n. \tag{22}$$

In the last two layers, defuzzification is made and the output of the network is calculated as:

$$\text{Output of Network} = \boldsymbol{f}_o = \frac{y}{\sum_{j=1}^{n} \mu_j}. \tag{23}$$

Therefore, the parameter vector $\boldsymbol{p}$ is defined as:

$$\boldsymbol{p} = [w_1, ..., w_n, c_{11}, c_{12}, ..., c_{mn}, \sigma_{11}, \sigma_{12}, ..., \sigma_{mn}, a_{11}, a_{12}, ..., a_{mn}, b_{11}, b_{12}, ..., b_{mn}, \theta_{11}, \theta_{12}, ..., \theta_{mn}]. \tag{24}$$

3.3. Cost function

To define an effective cost function to optimize by the RFWNN, two scenarios are considered. First, in a free task by the robotic manipulator, the velocity between the end-effector and the variable environment should be controlled

Please cite this article in press as: M.H. Hamedani et al., Recurrent fuzzy wavelet neural network variable impedance control of robotic manipulators with fuzzy gain dynamic surface in an unknown varied environment, Fuzzy Sets Syst. (2020), https://doi.org/10.1016/j.fss.2020.05.001

to prevent unstable behavior. However, in contact task, the force applied by the environment should converge to the desired value. Accordingly, a goal function for the learning of RFWNN can be defined as:

$$E(t) = \mu_v E_v(t) + \mu_f E_d(t)\,, \tag{25}$$

where μ_v and μ_f are gain functions which can be considered variable or constant. In addition, $E_v(t)$ and $E_f(t)$ can be defined as

$$E_v(t) = \frac{1}{2}\dot{\tilde{\boldsymbol{x}}}^T\dot{\tilde{\boldsymbol{x}}}\,, \tag{26}$$

$$E_f(t) = \frac{1}{2}\boldsymbol{e}_f{}^T\boldsymbol{e}_f\,. \tag{27}$$

In fact, the (26) and (27) evaluate velocity and force error. The weights of RFWNN need to be modified using a learning algorithm to minimize the cost function (25) and to enable the robotic manipulator to interact with the varied unknown environment.

3.4. Learning approach of RFWNN

The learning of the RFWNN is performed by modifying the weights of the network to optimize the cost function. To reach this aim, the gradient algorithm is considered to optimize the cost function in (25). The vector parameter p in (24) is adjusted using the following formula:

$$\boldsymbol{p}(t+1) = \boldsymbol{p}(t) - \gamma_i(1-\mu)\frac{\partial E}{\partial \boldsymbol{p}} + \mu(\boldsymbol{p}(t) - \boldsymbol{p}(t-1))\,, \qquad \mathbf{i} = \mathbf{1}, \mathbf{2}\,. \tag{28}$$

In order to update the weights of the network efficiency, two learning rates for the fuzzy and the wavelet sections are considered. Where γ_1 is the learning rate for w_n, c_{mn}, and σ_{mn} and, γ_2 is the learning rate for a_{mn}, b_{mn}, and θ_{mn}. Because E as the cost function is not explicitly the function of the $\boldsymbol{f}_o$ (the network output), the derivative $\frac{\partial E}{\partial \boldsymbol{p}}$ can be calculated by the following formulas:

$$\frac{\partial E}{\partial \boldsymbol{p}} = \frac{\partial E}{\partial \ddot{\boldsymbol{x}}_I}\frac{\partial \ddot{\boldsymbol{x}}_I}{\partial \boldsymbol{f}_o}\frac{\partial \boldsymbol{f}_o}{\partial \boldsymbol{p}}\,. \tag{29}$$

The term $\frac{\partial E}{\partial \ddot{\boldsymbol{x}}_I}$ can be expanded from Eq. (25) and (15) as:

$$\frac{\partial E}{\partial \ddot{\boldsymbol{x}}_I} = \mu_v\frac{\partial E_v}{\partial \dot{\tilde{\boldsymbol{x}}}}\frac{\partial \dot{\tilde{\boldsymbol{x}}}}{\partial \ddot{\boldsymbol{x}}_I} + \mu_f\frac{\partial E_f}{\partial \dot{\boldsymbol{e}}_f}\frac{\partial \dot{\boldsymbol{e}}_f}{\partial \ddot{\boldsymbol{x}}_I}\,, \tag{30}$$

$$\frac{\partial E}{\partial \ddot{\boldsymbol{x}}_I} = -\mu_v\dot{\tilde{\boldsymbol{x}}}\boldsymbol{B}_{d_c}^{-1}\boldsymbol{M}_{dc} + \mu_f\dot{\boldsymbol{e}}_f\boldsymbol{M}_{dc}\,. \tag{31}$$

The term $\frac{\partial \ddot{\boldsymbol{x}}_I}{\partial \boldsymbol{f}_o}$ can be calculated from (15) as:

$$\frac{\partial \ddot{\boldsymbol{x}}_I}{\partial \boldsymbol{f}_o} = -\boldsymbol{K}_s\,. \tag{32}$$

Finally, the term $\frac{\partial \boldsymbol{f}_o}{\partial \boldsymbol{p}}$ can be obtained by the back propagation learning method.

3.5. Fuzzy gain dynamic surface control

To remove the uncertainty and disturbance term (8), FGDS is proposed to tune the dynamic surface gain. In the first step, the virtual control law is designed for x_2 in the joint space. Therefore, the commended trajectory from (10) and (11) is considered in the joint space using the inverse kinematics. We denote $\boldsymbol{x}_{I1}$ and $\boldsymbol{x}_{I2}$ as the joint space variable for the commanded trajectory $\boldsymbol{z}_1$ and $\boldsymbol{z}_2$, respectively. For the present purpose, the first error surface is defined as:

$$\boldsymbol{s}_1 = \boldsymbol{x}_{R1} - \boldsymbol{x}_{I1}\,, \tag{33}$$

and its derivative is

Please cite this article in press as: M.H. Hamedani et al., Recurrent fuzzy wavelet neural network variable impedance control of robotic manipulators with fuzzy gain dynamic surface in an unknown varied environment, Fuzzy Sets Syst. (2020), https://doi.org/10.1016/j.fss.2020.05.001

$$\dot{s}_1 = x_{R2} - x_{I2}\,. \tag{34}$$

A virtual control $\bar{x}_2$ is designed to drive $s_1 \to 0$ as follows:

$$\bar{x}_2 = -K_1 s_1 + x_{I2}\,, \qquad K_1 > 0\,. \tag{35}$$

Because of multiple surface sliding control drawbacks [35], $\bar{x}_2$ is passed through a first order filter with time constant $\tau_2 > 0$ as:

$$\tau_2 \dot{x}_{2f} + x_{2f} = \bar{x}_2\,, \qquad x_{2f}(0) = \bar{x}_2(0)\,. \tag{36}$$

In the second step, the actual control law for τ is designed. Therefore, second error surface s_2, with filtering virtual control vector x_{2f} is defined as follows:

$$s_2 = x_{R2} - x_{2f}\,, \tag{37}$$

and its derivative is

$$\dot{s}_2 = \dot{x}_{R2} - \dot{x}_{2f}\,. \tag{38}$$

By substituting (7) and (36) in (38), it yields:

$$\dot{s}_2 = H(x_{R_1})^{-1}\{-V(x_{R_1}, x_{R_2}) - G(x_{R_1}) - J^T(x_{R_1})\mathbf{f_e} + \tau\} + \mathbf{U} - \frac{\bar{x}_2 - x_{2f}}{\tau_2}\,. \tag{39}$$

We now propose a signal control τ such that $s_2 \to 0$. As already mentioned, the control objective is to design a fuzzy gain dynamic surface control as an uncertainty and disturbance observer for the state vector x_{R1} and x_{R2} in order to track the desired state represented by x_{I1}, x_{I1}. Accordingly, the control signal is proposed as follows:

$$\tau = \{V(x_{R_1}, x_{R_2}) + G(x_{R_1}) + J^T(x_{R_1})\mathbf{f_e} + H(x_{\mathbf{R_1}})(-K_2 s_2 + \frac{\bar{x}_2 - x_{2f}}{\tau_2})\}\,. \tag{40}$$

Substituting (40) in (39) yields:

$$\dot{s}_2 = -K_2 s_2 + U\,. \tag{41}$$

Analytic expression of the closed-loop system is driven via surface errors (s_1 and s_2) and boundary layer error y_2. Substituting (37) in (34) yields:

$$\dot{s}_1 = s_2 + x_{2f} - x_{I2}\,. \tag{42}$$

Boundary layer error is defined as follows:

$$y_2 = x_{2f} - \bar{x}_2 = x_{2f} + K_1 s_1 - x_{I2}\,, \tag{43}$$

and its derivative is

$$\dot{y}_2 = \frac{\bar{x}_2 - x_{2f}}{\tau_2} + \dot{K}_1 s_1 + K_1 \dot{s}_1 - \dot{x}_{I2}\,. \tag{44}$$

Substituting (42) and (43) in (44) yields

$$\dot{y}_2 = \frac{\bar{x}_2 - x_{2f}}{\tau_2} + \dot{K}_1 s_1 + K_1 s_2 + K_1(x_{2f} - x_{I2}) - \dot{x}_{I2} = -\frac{y_2}{\tau_2} + R_2\,, \tag{45}$$

where $R_2 = \dot{K}_1 s_1 + K_1 s_2 + K_1(x_{2f} - x_{I2}) - \dot{x}_{I2}$. From equations (41), (42), and (43) dynamic surfaces can be rewritten as follows:

$$\dot{s}_1 = s_2 + y_2 - K_1 s_1\,, \tag{46}$$

$$\dot{s}_2 = -K_2 s_2 + U\,, \tag{47}$$

where (45)-(47) are the equations of the closed-loop system. In the proposed method, to remove the effects of uncertainty and disturbance term U in (47), the fuzzy gain dynamic surface method is presented to tune K_2 and K_1 gains. By adapting the value of the K_2 in (47), the effect of disturbance and uncertainty U can be removed. For instance, if

Please cite this article in press as: M.H. Hamedani et al., Recurrent fuzzy wavelet neural network variable impedance control of robotic manipulators with fuzzy gain dynamic surface in an unknown varied environment, Fuzzy Sets Syst. (2020), https://doi.org/10.1016/j.fss.2020.05.001

Table 2
Fuzzy rules to tune $\boldsymbol{K}_1$.

Rule No.	IF	THEN
$\mathbf{R_1}$	s_1 is Big Positive and $\dot{s}_1$ is Big Positive	$\boldsymbol{K}_1$ is Big Large
$\mathbf{R_2}$	s_1 is Big Positive and $\dot{s}_1$ is Small Negative	$\boldsymbol{K}_1$ is Large
$\mathbf{R_3}$	s_1 is Big Positive and $\dot{s}_1$ is Big Negative	$\boldsymbol{K}_1$ is Small
...	...	...
$\mathbf{R_n}$	s_1 is Small Negative and $\dot{s}_1$ is Big Positive	$\boldsymbol{K}_1$ is Big Small

the $\boldsymbol{U}$ exists, then by increasing the value of the $\boldsymbol{K}_2$ the effects of the $\boldsymbol{U}$ will be decreased. However, the big value gains make the spike response especially in transient response of the system and increase the noise effect. To prevent large sudden variations of torque motor signals, especially in transient response to the system, the gains of controllers $\boldsymbol{K}_1$ and $\boldsymbol{K}_2$ are selected by the following fuzzy rules in Table 2, where $\boldsymbol{s}_1$ and $\dot{\boldsymbol{s}}_1$ are obtained from (33) and (34), and $\boldsymbol{K}_1$ is the fuzzy gain and output of the fuzzy rules. Note that, if we decided to apply $\boldsymbol{s}_2$ as the input of the fuzzy rules then we had to also consider its rate ($\dot{\boldsymbol{s}}_2$). However, because of difficulty in measuring acceleration feedback (drift or noise drawbacks) in practice, $\dot{\boldsymbol{s}}_2$ is not available. In addition, the $\boldsymbol{U}$ in (47) affects the first dynamic surface implicitly. Therefore, $\boldsymbol{K}_2$ is not directly tuned by fuzzy rules and is proposed to consider by the $\boldsymbol{K}_2 = \delta \boldsymbol{K}_1$ and $\delta > 0$. Additionally, δ is chosen by the designer based on the knowledge of the system so that the magnitude of the control signal is acceptable.

Big Positive, Small Positive, Zero, Small Negative, Big Negative are considered as the linguistic terms of the primes part of the fuzzy rules and Big Large, Large, Medium, Small and Big Small are the linguistic terms of the consequence part. According to mentioned linguistic term for the fuzzy rules, all membership functions of their corresponding fuzzy sets are Gaussian functions such as:

$$\mu_m(x) = e^{-\frac{(x-c_m)^2}{2\sigma_m^2}}, \tag{48}$$

where x is the input of the membership function and takes $\boldsymbol{s}_1$ and $\dot{\boldsymbol{s}}_1$. Additionally, m is used to distinguish the membership function for each of the linguistic terms. For example for the membership function for the term of the Small Negative for $\dot{\boldsymbol{s}}_1$ in the second rule can be considered as $\mu_{smallNegative}(\dot{s}_1) = e^{-\frac{(\dot{s}_1 - c_{smallNegative})^2}{2\sigma^2_{smallNegative}}}$. The parameters of c_m and σ_m in (48) are chosen based on the knowledge about the constrained robot and controlling of the manipulator.

3.6. Stability analysis

The block diagram of the proposed controller for a robot manipulator is depicted in Fig. 4. The presented approach includes two closed loops. The outer loop is related to the variable impedance and the inner loop is considered for the fuzzy gain dynamic surface. The controller is proposed to force the robot manipulator to track the variable impedance control (9) and to remove the uncertainty and disturbance (8).
The variable impedance block is responsible for determining the desired state vector z_1 as position of the reference trajectory. Fuzzy gain block, based on the inputs, determines $\boldsymbol{K}_1$ and $\boldsymbol{K}_2$ to remove uncertainty and disturbance term U. Virtual control and first order filter generate $\bar{\boldsymbol{x}}_2$ and $\boldsymbol{x}_{2f}$, respectively. In addition, RFWNN block is responsible for providing $\boldsymbol{f}_o$ as an adaptive parameter of variable impedance block. Finally, proposed control signal is available for actuators of robot manipulator by actual control block.

The objective of the variable impedance control is to achieve a stability behavior and vibration reduction, which force the robot to have an acceptable interaction with the varied environment. By multiplying (9) by the error velocity $\dot{\tilde{\boldsymbol{x}}}^T$, we have

$$\dot{\tilde{\boldsymbol{x}}}^T \boldsymbol{M}_d \ddot{\tilde{\boldsymbol{x}}} = -\dot{\tilde{\boldsymbol{x}}}^T \boldsymbol{e}_f - \dot{\tilde{\boldsymbol{x}}}^T \boldsymbol{B}_d \dot{\tilde{\boldsymbol{x}}} - \dot{\tilde{\boldsymbol{x}}}^T \boldsymbol{K}_d \tilde{\boldsymbol{x}} \tag{49}$$

$$\frac{dK}{dt} = -\dot{\tilde{\boldsymbol{x}}}^T \boldsymbol{e}_f - \dot{\tilde{\boldsymbol{x}}}^T \boldsymbol{B}_d \dot{\tilde{\boldsymbol{x}}} - \frac{dP}{dt}, \tag{50}$$

where K is the kinetic energy, and P refers to potential energy. In order to guarantee the passivity of the impedance profile and stability of the system, the kinetic energy must not be increased; namely, $\frac{dK}{dt} \leq 0$. The damping term

Please cite this article in press as: M.H. Hamedani et al., Recurrent fuzzy wavelet neural network variable impedance control of robotic manipulators with fuzzy gain dynamic surface in an unknown varied environment, Fuzzy Sets Syst. (2020), https://doi.org/10.1016/j.fss.2020.05.001

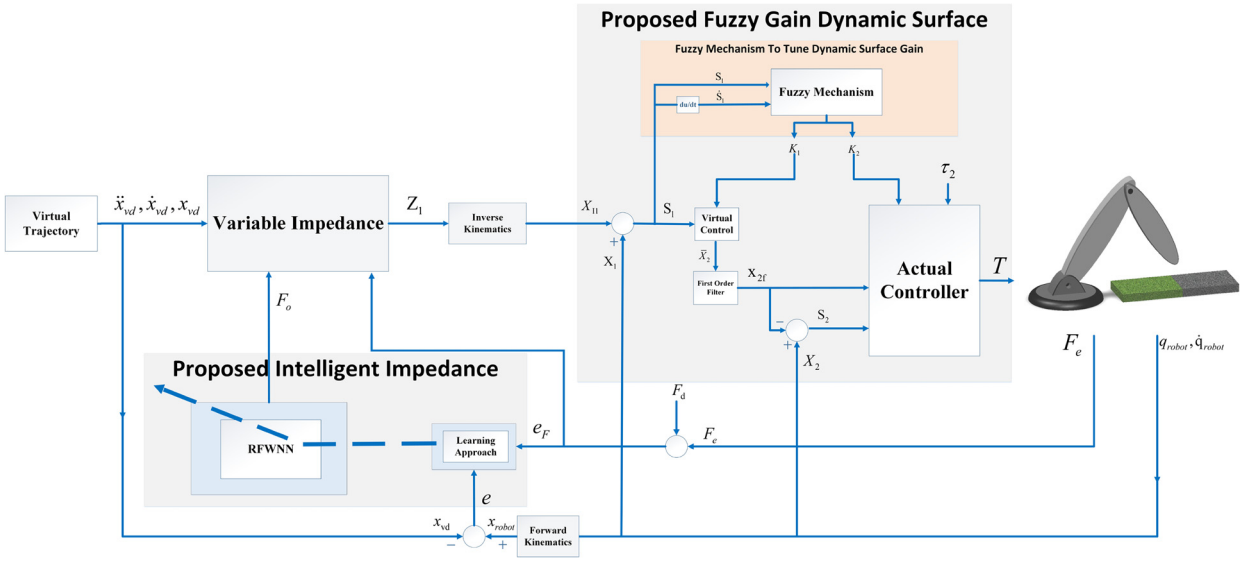

Fig. 4. Block diagram of the proposed controller for a robot manipulator.

$-\dot{\tilde{\boldsymbol{x}}}^T \boldsymbol{B}_d \dot{\tilde{\boldsymbol{x}}} < 0, \forall \dot{\tilde{\boldsymbol{x}}} \neq 0$ leads to permanent decrease in the kinetic energy. According to (50), to guarantee the reduction of the kinetic energy K, the potential energy P has to increase for all time instants; namely, $\frac{dP}{dt} > 0, \forall t \geq 0$. However, it is not possible to realize in a passive impedance and it depends on the selection of the impedance parameters. For example, by choosing the impedance parameters $\boldsymbol{B}_d$, $\boldsymbol{K}_d$, and $\boldsymbol{M}_d$ such that the condition $\frac{\boldsymbol{B}_d}{2\sqrt{\boldsymbol{K}_d \boldsymbol{M}_d}} < 1$ is complied, it can be proved that there exists a time period with $\frac{dP}{dt} = \dot{\tilde{\boldsymbol{x}}}^T \boldsymbol{K}_d \tilde{\boldsymbol{x}} < 0$ which it leads to the sign of $\frac{dK}{dt}$ cannot be defined and predictable. Therefore, considering the stability of the impedance profile is important when the parameters of the impedance are variable.

In the following, Theorems 1 and 2 are presented to guarantee the stability closed-loop system.

Theorem 1. *Consider closed-loop system Fig. 4 and the robot manipulator (1). Let $\boldsymbol{M}_d(t)$, $\boldsymbol{B}_d(t)$ and $\boldsymbol{K}_d(t)$ be symmetric, positive definite and continuously differentiable varying inertial, damping and stiffness profiles, respectively. Then, the closed loop system in 4 is uniformly ultimately bounded (UUB) if the following control torque is applied:*

$$\boldsymbol{\tau} = \{\boldsymbol{V}(\boldsymbol{x}_{R_1}, \boldsymbol{x}_{R_2}) + \boldsymbol{G}(\boldsymbol{x}_{R_1}) + \boldsymbol{J}^T(\boldsymbol{x}_{R_1})\mathbf{f_e} + \boldsymbol{H}(\boldsymbol{x}_{\mathbf{R_1}})(-\boldsymbol{K_2 s_2} + \frac{\bar{\boldsymbol{x}}_{\mathbf{2}} - \boldsymbol{x}_{\mathbf{2f}}}{\tau_2})\} \tag{51}$$

where $\boldsymbol{K}_2$ is selected by the fuzzy mechanism. Additionally, Assumption 2 and the following conditions should be satisfied:

$$\begin{aligned} &\boldsymbol{K}_1(t) \geq 2 + \boldsymbol{K}_1^*, \boldsymbol{K}_2(t) \geq \frac{5}{4} + \boldsymbol{K}_2^*, \text{ and } \frac{1}{\tau_2} \geq \frac{5}{4} + \lambda_2 \\ &\text{where } \boldsymbol{K}_1^* > 0, \boldsymbol{K}_2^* > 0, \lambda_2 > 0, \text{ and} \end{aligned} \tag{52}$$

$$\boldsymbol{K}_s(t) = \begin{cases} k_s & \dot{\tilde{\boldsymbol{x}}} \boldsymbol{f}_o \geq 0 \\ k_s & \dot{\tilde{\boldsymbol{x}}} \boldsymbol{f}_o < 0 \text{ and } |\dot{\tilde{\boldsymbol{x}}}^T k_s \boldsymbol{f}_o| < \dot{\tilde{\boldsymbol{x}}}^T \boldsymbol{B}_{dc} \dot{\tilde{\boldsymbol{x}}} \\ 0 & \dot{\tilde{\boldsymbol{x}}} \boldsymbol{f}_o < 0 \text{ and } |\dot{\tilde{\boldsymbol{x}}}^T k_s \boldsymbol{f}_o| \geq \dot{\tilde{\boldsymbol{x}}}^T \boldsymbol{B}_{dc} \dot{\tilde{\boldsymbol{x}}}. \end{cases} \tag{53}$$

Proof. To prove the stability of the closed loop system in Fig. 4, it is necessary to consider the variable impedance and fuzzy gain dynamic surface in the stability procedure. Proving the stability of the dynamic surface with time varying gain is required because the proposed fuzzy gain dynamic surface is applied to force the robot to track the desired impedance. Furthermore, because of the presented intelligent impedance, the desired impedance (9) is a linear

Please cite this article in press as: M.H. Hamedani et al., Recurrent fuzzy wavelet neural network variable impedance control of robotic manipulators with fuzzy gain dynamic surface in an unknown varied environment, Fuzzy Sets Syst. (2020), https://doi.org/10.1016/j.fss.2020.05.001

time-varying system and therefore, the stability of (9) is required to be considered. According to the proof mentioned above, the Lyapunov function is chosen as:

$$V = V_{DS} + V_I \,, \tag{54}$$

where

$$V_{DS} = \frac{1}{2}[\boldsymbol{s}_1^T \boldsymbol{s}_1 + \boldsymbol{s}_2^T \boldsymbol{s}_2 + \boldsymbol{y}_2^T \boldsymbol{y}_2] \,, \tag{55}$$

$$V_I = \frac{1}{2}[\dot{\tilde{\boldsymbol{x}}}^T \boldsymbol{M}_{dc} \dot{\tilde{\boldsymbol{x}}} + \tilde{\boldsymbol{x}}^T \boldsymbol{K}_{dc} \tilde{\boldsymbol{x}}] \,. \tag{56}$$

V_{DS} is used to analyze the stability of the fuzzy gain dynamic surface and V_I can be used for varying impedance control. Differentiating (55) with respect to time and substituting (46) and (47) yields

$$\begin{aligned} \dot{V}_{DS} &= \boldsymbol{s}_1^T \dot{\boldsymbol{s}}_1 + \boldsymbol{s}_2^T \dot{\boldsymbol{s}}_2 + \boldsymbol{y}_2^T \dot{\boldsymbol{y}}_2 \\ &= \boldsymbol{s}_1^T (\boldsymbol{s}_2 + \boldsymbol{y}_2 - \boldsymbol{K}_1 \boldsymbol{s}_1) + \boldsymbol{s}_2^T (-\boldsymbol{K}_2 \boldsymbol{s}_2 + \boldsymbol{U}) + \boldsymbol{y}_2^T (-\frac{\boldsymbol{y}_2}{\tau_2} + R_2) \,. \end{aligned} \tag{57}$$

It is obvious that,

$$\begin{aligned} \dot{V}_{DS} &\le \|\boldsymbol{s}_1\| \|\boldsymbol{s}_2\| + \|\boldsymbol{s}_1\| \|\boldsymbol{y}_2\| - \boldsymbol{K}_1 \|\boldsymbol{s}_1\|^2 - \boldsymbol{K}_2 \|\boldsymbol{s}_2\|^2 \\ &\quad + \|\boldsymbol{s}_2\| \boldsymbol{U} - \frac{\|\boldsymbol{y}_2\|^2}{\tau_2} + |\boldsymbol{y}_2^T R_2| \,. \end{aligned} \tag{58}$$

For any finite workspace Ω, similar Assumption 1 and boundedness of x_d, there exists a positive constant P_2 such that $\|R_2\| \le P_2$. Using the fact that $2a_1a_2 \le a_1^2 + a_2^2$, (i.e. $\|S_1\| \|S_2\| = 2\|S_1\| \frac{\|S_2\|}{2} \le \|S_1\|^2 + \frac{\|S_2\|^2}{4}$)

$$\begin{aligned} \dot{V}_{DS} &\le \|\boldsymbol{s}_1\|^2 + \frac{\|\boldsymbol{s}_2\|^2}{4} + \|\boldsymbol{s}_1\|^2 + \frac{\|\boldsymbol{y}_2\|^2}{4} - \boldsymbol{K}_1 \|\boldsymbol{s}_1\|^2 - \boldsymbol{K}_2 \|\boldsymbol{s}_2\|^2 \\ &\quad + \|\boldsymbol{s}_2\|^2 - \frac{\|\boldsymbol{y}_2\|^2}{\tau_2} + \|\boldsymbol{y}_2\|^2 + \frac{\boldsymbol{P}_2^2}{4} + \frac{\delta^2}{4} \,. \end{aligned} \tag{59}$$

In order to $\dot{V}_{DS} \le 0$, we choose $\boldsymbol{K}_1(t) = 2 + \boldsymbol{K}_1^*$, $\boldsymbol{K}_2(t) = \frac{5}{4} + \boldsymbol{K}_2^*$ and $\frac{1}{\tau_2} = \frac{5}{4} + \lambda_2$ and substituting into (59) yields

$$\begin{aligned} \dot{V}_{DS} &\le -\boldsymbol{K}_1^* \|\boldsymbol{s}_1\|^2 - \boldsymbol{K}_2^* \|\boldsymbol{s}_2\|^2 - \lambda_2 \|\boldsymbol{y}_2\|^2 + \frac{\delta^2}{4} + \frac{\boldsymbol{P}_2^2}{4} \\ &\le -\boldsymbol{K}_1^* \|\boldsymbol{s}_1\|^2 - \boldsymbol{K}_2^* \|\boldsymbol{s}_2\|^2 - \lambda_2 \|\boldsymbol{y}_2\|^2 + H \,, \end{aligned} \tag{60}$$

where $\boldsymbol{K}_1^* > 0$, $\boldsymbol{K}_2^* > 0$; statement H is the high order term which introduces the uncertainty presence. Let us choose constant ς satisfying the condition as follows:

$$0 < \varsigma < min[\boldsymbol{K}_1^*, \boldsymbol{K}_2^*, \lambda_2] \,. \tag{61}$$

Hence, we obtain:

$$\dot{V}_{DS} \le -2\varsigma \big(\frac{1}{2}(\|\boldsymbol{s}_1\|^2 + \|\boldsymbol{s}_2\|^2 + \|\boldsymbol{y}_2\|^2)\big) + H = -2\varsigma V_{DS} + H \,. \tag{62}$$

(62) implies that $\dot{V}_{DS} < 0$ when $V_{DS} > \frac{H}{2\varsigma}$. The surface errors ($\boldsymbol{s}_1$ and $\boldsymbol{s}_2$) and the boundary layer error $\boldsymbol{y}_2$ are all uniformly ultimately bounded in a compact set which is proved in Theorem 2. Now, differentiating (56) with respect to time yields:

$$\dot{V}_I = \dot{\tilde{\boldsymbol{x}}}^T \boldsymbol{M}_{dc} \ddot{\tilde{\boldsymbol{x}}} + \tilde{\boldsymbol{x}}^T \boldsymbol{K}_{dc} \dot{\tilde{\boldsymbol{x}}} \,, \tag{63}$$

and substituting (14) in (63) yields:

$$\dot{V}_I = -\dot{\tilde{\boldsymbol{x}}}^T (\boldsymbol{B}_{dc} \dot{\tilde{\boldsymbol{x}}} + \boldsymbol{K}_{dc} \tilde{\boldsymbol{x}} + \boldsymbol{K}_s \boldsymbol{f}_o) + \tilde{\boldsymbol{x}}^T \boldsymbol{K}_{dc} \dot{\tilde{\boldsymbol{x}}} \,, \tag{64}$$

$$\dot{V}_I = -\dot{\tilde{\boldsymbol{x}}}^T \boldsymbol{B}_{dc} \dot{\tilde{\boldsymbol{x}}} - \dot{\tilde{\boldsymbol{x}}}^T \boldsymbol{K}_s \boldsymbol{f}_o \,. \tag{65}$$

Please cite this article in press as: M.H. Hamedani et al., Recurrent fuzzy wavelet neural network variable impedance control of robotic manipulators with fuzzy gain dynamic surface in an unknown varied environment, Fuzzy Sets Syst. (2020), https://doi.org/10.1016/j.fss.2020.05.001

In (65), $\boldsymbol{K}_s(t) \geq 0$ is positive. However, the sign of the $\dot{\tilde{\boldsymbol{x}}}^T$ and $\boldsymbol{f}_o$ is not definite. Consequently, the term $\dot{\tilde{\boldsymbol{x}}}^T \boldsymbol{K}_s \boldsymbol{f}_o$ has the potential to make $\dot{V}_I > 0$. Therefore, we consider the $\boldsymbol{K}_s$ as a design parameter to guarantee the stability of the system using (53).

In order that $\dot{V}_I < 0$ and to guarantee the stability of impedance profile, we consider $\boldsymbol{K}_s(t) = 0$ for the condition $\dot{\tilde{\boldsymbol{x}}}^T \boldsymbol{f}_o < 0$ and $|\dot{\tilde{\boldsymbol{x}}}^T k_s \boldsymbol{f}_o| \geq \dot{\tilde{\boldsymbol{x}}}^T \boldsymbol{B}_{dc} \dot{\tilde{\boldsymbol{x}}}$. In fact, by observing the power $\dot{\tilde{\boldsymbol{x}}}^T \boldsymbol{f}_o < 0$ generated by RFWNN, the stabilizer $\boldsymbol{K}_s(t)$ decides that it is allowed to injected to system or not. In fact, (53) is working as a switching condition to guarantee $\dot{V}_I < 0$ in (65). Consequently, according to (62) which implies that $\dot{V}_{DS} < 0$ when $V_{DS} > \frac{H}{2\varsigma}$ and constraint (65), $\dot{V} = \dot{V}_{DS} + \dot{V}_I < 0$ then the proof of Theorem 1 is thus established.

Now, Theorem. 2 is presented to verify that error vector bounds for proposed control system converge asymptotically to a compact set. □

Theorem 2. *According to* (45), (46), (47), *and considering* V_{DS} *in Theorem. 1, error vectors including surface errors, boundary layer errors and estimation errors are defined as follows:*

$$\boldsymbol{N} = \begin{bmatrix} \boldsymbol{s}_1^T & \boldsymbol{s}_2^T & \boldsymbol{y}_2^T \end{bmatrix}.$$

$\boldsymbol{N}$ *converges asymptotically to the compact set*

$$\Omega_N := \{\boldsymbol{N} \in \mathbb{R}^{l_N \times 1} | \|\boldsymbol{N}\| \leq \sqrt{M}\}, \tag{66}$$

where $M = 2(V_{DS}(0)e^{-2\varsigma t} + \frac{H}{2\varsigma})$ *with* ς *and* H *are given in* (60) *and* (61).

Proof. Multiplying (62) by $e^{2\varsigma t}$ yields

$$\frac{d(V_{DS}e^{2\varsigma t})}{dt} \leq He^{2\varsigma t} \tag{67}$$

Integrating (67) and multiplying by $e^{-2\varsigma t}$, we have

$$V_{DS}(t) \leq V_{DS}(0)e^{-2\varsigma t} - \frac{H}{2\varsigma}e^{-2\varsigma t} + \frac{H}{2\varsigma}, \tag{68}$$

and $\frac{H}{2\varsigma}e^{-2\varsigma t} \to 0$ and then

$$V_{DS}(t) \leq V_{DS}(0)e^{-2\varsigma t} + \frac{H}{2\varsigma}. \tag{69}$$

According to (55) and $\boldsymbol{N}$, we have

$$\frac{1}{2}\boldsymbol{N}^T\boldsymbol{N} \leq V_{DS}(0)e^{-2\varsigma t} + \frac{H}{2\varsigma}. \tag{70}$$

Now, we can obtain:

$$\|\boldsymbol{N}\| \leq \sqrt{M}, \tag{71}$$

where $M = 2(V_{DS}(0)e^{-2\varsigma t} + \frac{H}{2\varsigma})$. Therefore, if $t = 0$ then $\|\boldsymbol{N}\| \leq 2(V_{DS}(0) + \frac{H}{2\varsigma})$. If $t \to \infty$ then $V_{DS}(0)e^{-2\varsigma t} \to 0$ and $\|\boldsymbol{N}\| \leq \frac{H}{2\varsigma}$. Consequently, the compact set is introduced as follows:

$$F = \{\boldsymbol{s}_1, \boldsymbol{s}_2, \boldsymbol{y}_2 \mid \|\boldsymbol{s}_1\|^2 + \|\boldsymbol{s}_2\|^2 + \|\boldsymbol{y}_2\|^2 \leq \frac{H}{\varsigma}\}. \tag{72}$$

Compact set F can be kept arbitrarily small choosing $\boldsymbol{K}_1^*$, $\boldsymbol{K}_2^*$ and λ_2. As a result, $\boldsymbol{s}_1$, $\boldsymbol{s}_2$ and $\boldsymbol{y}_2$ as the states of the closed loop system are uniformly ultimately bounded and converge to the compact set F. □

Please cite this article in press as: M.H. Hamedani et al., Recurrent fuzzy wavelet neural network variable impedance control of robotic manipulators with fuzzy gain dynamic surface in an unknown varied environment, Fuzzy Sets Syst. (2020), https://doi.org/10.1016/j.fss.2020.05.001

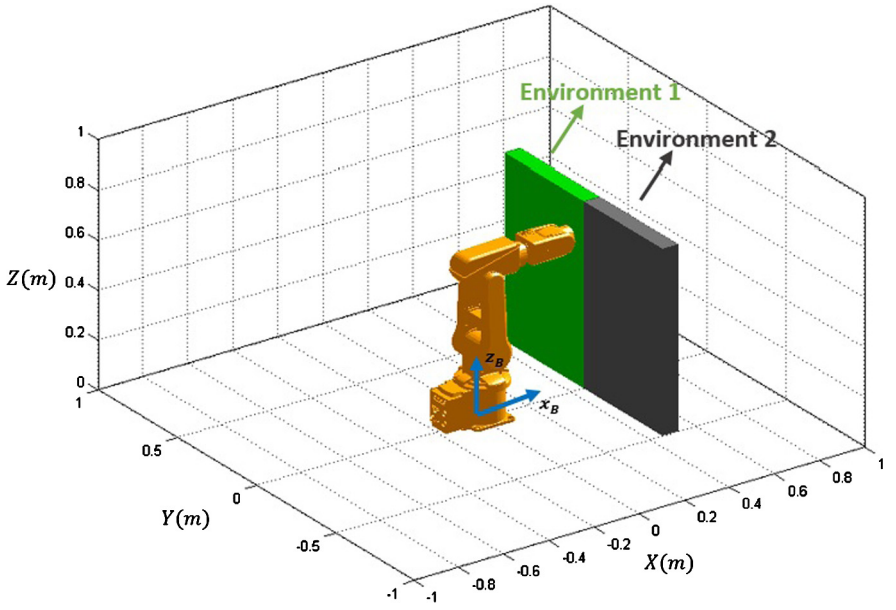

Fig. 5. ABB IRB 120 robot manipulator and the wall position, the green wall is considered a known environment and black wall is considered an unknown varied environment. (For interpretation of the colors in the figure(s), the reader is referred to the web version of this article.)

4. Simulation study

To illustrate the effectiveness and robustness of the proposed controller including the intelligent variable impedance and fuzzy gain dynamic surface, a set of simulations with large input disturbances and varied environments is presented. Additionally, to focus on the structure of the control aspects, the model of the ABB IRB120 robot is designed as a simulator with six revolute joints as shown in Fig. 5. IRB 120 manipulator one of the portable robot because it has only 25 kg weight. In this work, we design a simulator using MATLAB 2014a to generate and insert the desired objects including robot manipulator and interactive environment. In order to use the simulator, the CAD model of the objects need to be saved as the STL format and then became a ".mat" file by a MATLAB interface code. Let m_i and l_i be the mass of link i, lc_i be the distance from joint $i-1$ to the center of the mass of the link i and I_i be the moment of inertia of the link i about an axis coming out of the page passing through the center of mass of link i, $i = 1...6$. In addition, Fig. 6 depicts the coordinate system of ABB IRB 120 robot manipulator.

Generalized coordinates are defined to describe the dynamic equations of the robot as follows:

$$q = \begin{bmatrix} q_1 & q_2 & q_3 & q_4 & q_5 & q_6 \end{bmatrix}^T = \begin{bmatrix} \theta_1 & \theta_2 & \theta_3 & \theta_4 & \theta_5 & \theta_6 \end{bmatrix}^T . \tag{73}$$

The dynamics of the robot in joint space can be expressed as (1). Table 3 shows the parameters of the robot dynamical model of IRB120 manipulator.

The end-effector of the manipulator moves along a virtual desired position $\boldsymbol{x}_d$ depicted in Fig. 7 as follows:

The wall is located at $x_w = 0.45$, $-0.5 \leq y_w \leq 0.5$ and $0 \leq z_w \leq 0.72$. The initial conditions are set to be $q_0 = (0 \quad 0.06 \quad 0.7 \quad 0 \quad 0 \quad 0)^T$ rad and $\dot{q}_0 = (0 \quad 0 \quad 0 \quad 0 \quad 0 \quad 0)^T$ rad/s. To simulate the variable environment, we supposed that the environment applies the external force on the end-effector as follows:

$$\boldsymbol{f}_e(t) = \begin{bmatrix} f_{ex} \\ f_{ey} \\ f_{ez} \end{bmatrix} = \begin{cases} 8000 \begin{bmatrix} x - x_w \\ 0 \\ 0 \end{bmatrix} & -0.5 \leq y < 0 \text{ (Environment 1)} \\ (8000 + k_v \sin(\frac{2\pi}{0.3} y)) \begin{bmatrix} x - x_w \\ 0 \\ 0 \end{bmatrix} & 0 \leq y < 0.5 \text{ (Environment 2).} \end{cases} \tag{74}$$

Please cite this article in press as: M.H. Hamedani et al., Recurrent fuzzy wavelet neural network variable impedance control of robotic manipulators with fuzzy gain dynamic surface in an unknown varied environment, Fuzzy Sets Syst. (2020), https://doi.org/10.1016/j.fss.2020.05.001

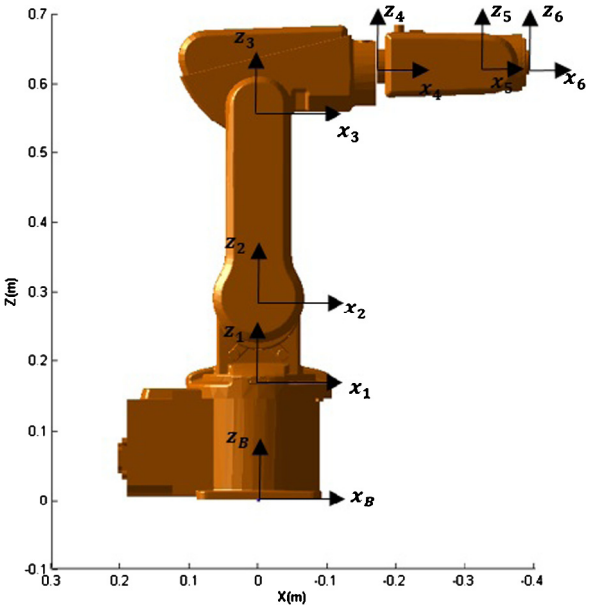

Fig. 6. Coordinate systems of ABB IRB 120 robot manipulator.

Table 3
Parameters of ABB robot manipulator.

PARAMETER	VALUE	UNIT
m_1	3	kg
m_2	3.9	kg
m_3	2.9	kg
m_4	1.3	kg
m_5	0.55	kg
m_6	0.014	kg
l_{c1}	$[0 \quad 0 \quad 0.062]^T$	m
l_{c2}	$[0 \quad 0 \quad 0.12]^T$	m
l_{c3}	$[0.5 \quad 0 \quad 0.03]^T$	m
l_{c4}	$[0 \quad 0 \quad 0.07]^T$	m
l_{c5}	$[0 \quad 0 \quad 0.03]^T$	m
l_{c6}	$[0 \quad 0 \quad 0]^T$	m
I_1	$Diag(0.014,0.01,0.014)$	kgm^2
I_2	$Diag(0.06,0.026,0.042)$	kgm^2
I_3	$Diag(0.008,0.013,0.017)$	kgm^2
I_4	$Diag(0.003,0.005,0.004)$	kgm^2
I_5	$Diag(0.0004,0.0008,0.0009)$	kgm^2
I_6	$Diag(0.002,0.002,0.003)$	kgm^2

The $k_v \sin(\frac{2\pi}{0.3}y)$ is known as the variable stiffness term of environment 2 where $K_v = 4000$. According to Fig. 5, the coordinate of environments 1 and 2 are $-0.5 \leq y < 0$ and $0 \leq y < 0.5$, respectively. Due to the wall position, end-effector tracks the virtual constraint surface $\boldsymbol{x}_d$ in the free space and moves sliding along the wall when it contacts the vertical wall. Fig. 8 shows the stiffness profiles of environments 1 and

In the following, two cases are considered to evaluate the performance of the proposed controller. Initially, fuzzy gain dynamic surface is presented to control the robot manipulator (Case 1). In case 1 and by a considering large and nonlinear disturbance, the performance of the proposed method and constant gain dynamic surface are compared. To evaluate only the structure of the fuzzy gain dynamic surface, in case 1, the parameters of the impedance are fixed as:

$$\boldsymbol{M}_d = diag\begin{bmatrix}2 & 2 & 2\end{bmatrix}^T \quad \boldsymbol{B}_d = diag\begin{bmatrix}300 & 300 & 300\end{bmatrix}^T \quad \boldsymbol{K}_d = diag\begin{bmatrix}50 & 50 & 50\end{bmatrix}^T \tag{75}$$

Please cite this article in press as: M.H. Hamedani et al., Recurrent fuzzy wavelet neural network variable impedance control of robotic manipulators with fuzzy gain dynamic surface in an unknown varied environment, Fuzzy Sets Syst. (2020), https://doi.org/10.1016/j.fss.2020.05.001

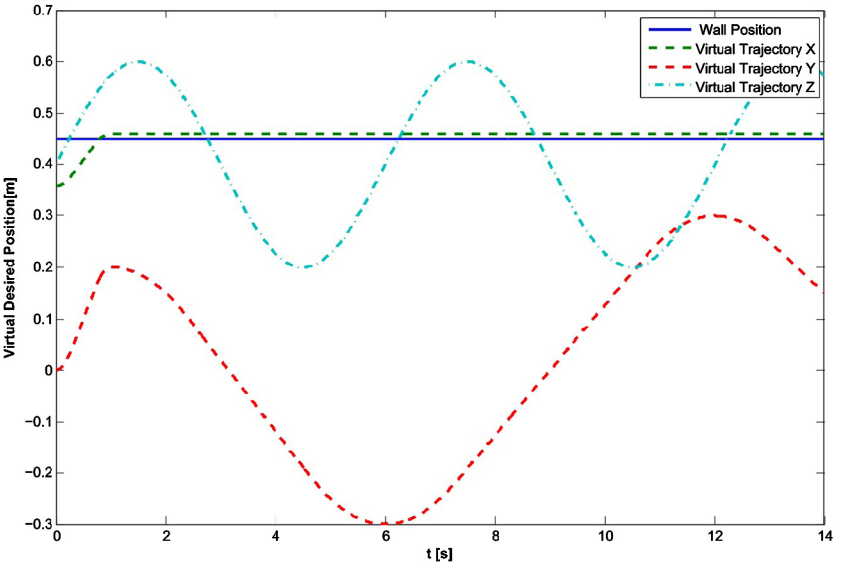

Fig. 7. Virtual desired $\boldsymbol{x}_d$ and the wall position.

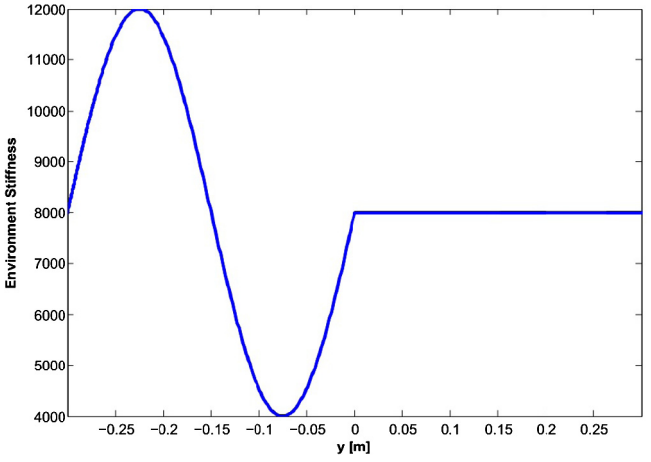

Fig. 8. Stiffness profiles for environments 1, 2 and free motion.

In addition, $\boldsymbol{f}_d$ is supposed as follows:

$$\boldsymbol{f}_d = \begin{bmatrix} f_{dx} \\ f_{dy} \\ f_{dz} \end{bmatrix} = \begin{bmatrix} 50 \\ 0 \\ 0 \end{bmatrix}. \tag{76}$$

In case 2, the performance of the proposed intelligent impedance control is evaluated by the varied unknown environment, and the results are discussed.

4.1. Case 1: proposed fuzzy gain dynamic surface

The main purpose of this simulation in case 1 is to evaluate the performance of the proposed method to handle the disturbances. Accordingly, the disturbance is described as follows:

Please cite this article in press as: M.H. Hamedani et al., Recurrent fuzzy wavelet neural network variable impedance control of robotic manipulators with fuzzy gain dynamic surface in an unknown varied environment, Fuzzy Sets Syst. (2020), https://doi.org/10.1016/j.fss.2020.05.001

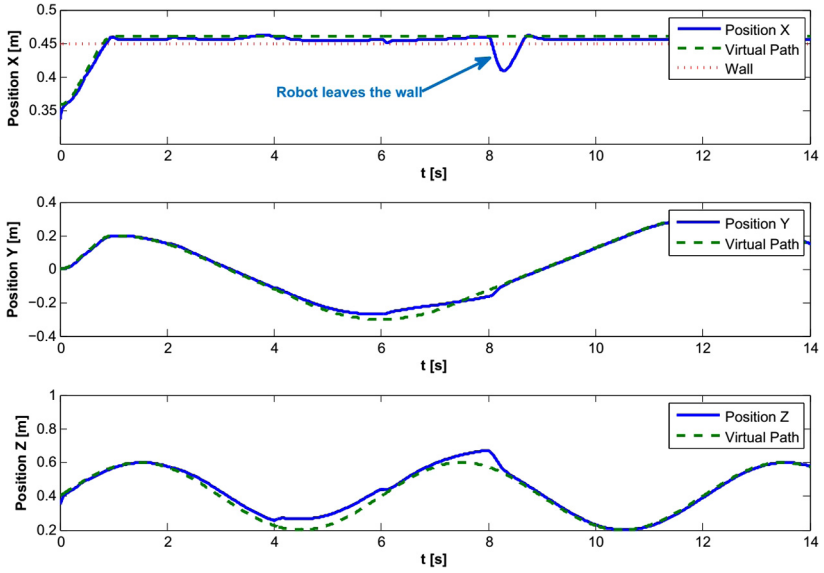

Fig. 9. Position tracking (Case 1.1).

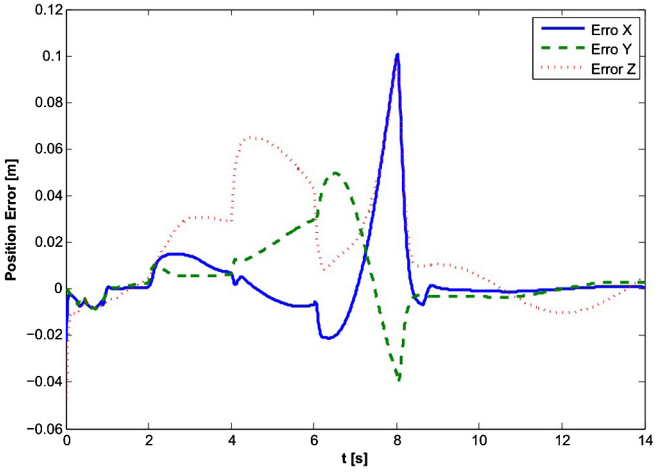

Fig. 10. Error Position tracking (Case 1.1).

$$\tilde{\boldsymbol{f}}(t) = \begin{cases} [10 \quad 10 \quad 10]^T & 2 \le t \le 4s \\ [25 \quad 25 \quad 25]^T & 4 \le t \le 6s \\ [45\sin(t) \quad 45\cos(t) \quad 45\sin(t)]^T & 6 \le t \le 8s \\ [0 \quad 0 \quad 0]^T & \text{otherwise}. \end{cases} \tag{77}$$

$\tilde{\boldsymbol{f}}(t)$ includes the fixed, variable and large nonlinear terms to demonstrate the ability of the proposed robust controller to handle the different types of disturbances.

Case 1.1: To establish a fair comparison, the gains for the dynamic surface $\boldsymbol{K}_1 = diag[36.3, 12, 12, 36.3, 36.3, 36.3]$ and $\boldsymbol{K}_2 = \boldsymbol{K}_1$ are considered the constant gains dynamic surface diagonal matrix such that the averages of the fuzzy gain and fixed gain are approximately equal. Fig. 9, Fig. 10 and Fig. 11 show the position tracking, error position and control signals of the robot in the presence of the disturbances (77), respectively. As it can be observed from Fig. 9 and Fig. 10, the position tracking is not satisfied when the disturbances are applied to the system. In Fig. 9, the manipulator leaves the wall during $8 - 9$ sec; therefore, the interaction between the robot and environment is lost.

Please cite this article in press as: M.H. Hamedani et al., Recurrent fuzzy wavelet neural network variable impedance control of robotic manipulators with fuzzy gain dynamic surface in an unknown varied environment, Fuzzy Sets Syst. (2020), https://doi.org/10.1016/j.fss.2020.05.001

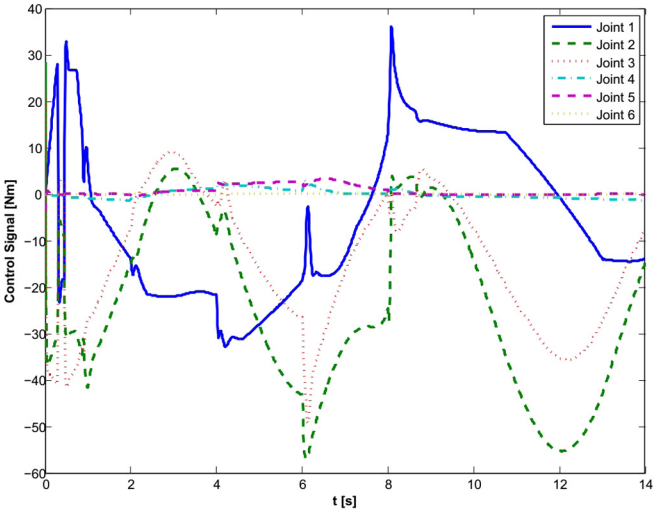

Fig. 11. Torque control signal (Case 1.1).

Table 4
Fuzzy rules designed for $\boldsymbol{K}_1$.

K_1 (Fuzzy Output)		S_1 (Fuzzy Input)				
		BN	**SN**	**Z**	**SP**	**BP**
$\dot{S}_1$ (Fuzzy Input)	**BN**	BL	L	M	BS	S
	SN	L	M	S	S	L
	Z	M	S	BS	S	M
	SP	L	S	S	M	L
	BP	S	BS	M	L	BL

Table 5
RMS of the position errors and force signal of the Cases 1 and 2.

Signal / Method	Position Error X(m) (RMS)	Position Error Y(m) (RMS)	Position Error Z(m) (RMS)
Constant Gain DSC (Case 1.1)	0.0182	0.0160	0.0306
Proposed Fuzzy Gain DSC (Case 1.2)	0.0044	0.0061	0.0110

Case 1.2: To demonstrate the proposed controller effectiveness to remove and handle the large and nonlinear disturbances effects, the proposed fuzzy gain dynamic surface is applied for the manipulator in Fig. 5. According to fuzzy set rules, the fuzzy rules for $\boldsymbol{K}_1$ are designed as in Table 4. In addition, $\boldsymbol{K}_2 = \delta \boldsymbol{K}_1$ and $\delta = 1$ is selected in this simulation, where BN, SN, Z, SP and BP are big negative, small negative, zero, small positive and big positive label linguistics for the fuzzy rules, respectively. In addition, BL, L, M, BS and S are big large, large, medium, big small and small, respectively. The position tracking, path following simulator and error position tracking are depicted in Fig. 12, Fig. 13 and Fig. 14, respectively. Fig. 12 and Fig. 14 show that the behavior of the end-effector position is acceptable in the face of the varied environment and disturbance. Additionally, the manipulator would be able to track the desired trajectory recommended by the impedance profile without leaving the wall. Furthermore, the snapshots of the manipulator performed by the designed simulator are depicted in Fig. 13. From Fig. 15 and practical point of view, the control torque signals are limited in the acceptable bound without saturation. From Fig. 16, $\boldsymbol{K}_1$ as a dynamic surface gain is changed by the fuzzy rules to improve the performance of the manipulator when the disturbances are applied. Consequently, the proposed fuzzy gain dynamic surface is able to remove the disturbances of (77).

Table 5 provides the Root Mean Square (RMS) of the position error and force error signal of cases 1. This reveals that the proposed method improves the position errors (RMS).

Please cite this article in press as: M.H. Hamedani et al., Recurrent fuzzy wavelet neural network variable impedance control of robotic manipulators with fuzzy gain dynamic surface in an unknown varied environment, Fuzzy Sets Syst. (2020), https://doi.org/10.1016/j.fss.2020.05.001

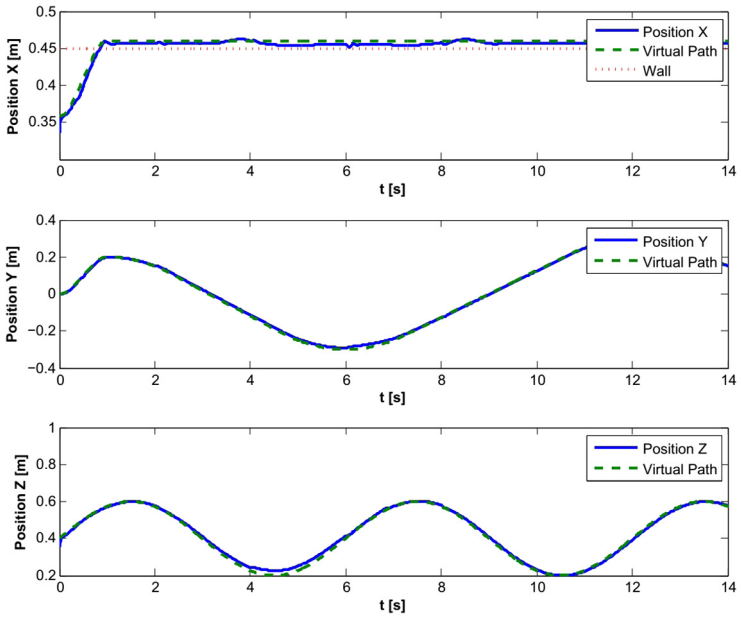

Fig. 12. Position tracking for proposed fuzzy gain dynamic surface (Case 1.2).

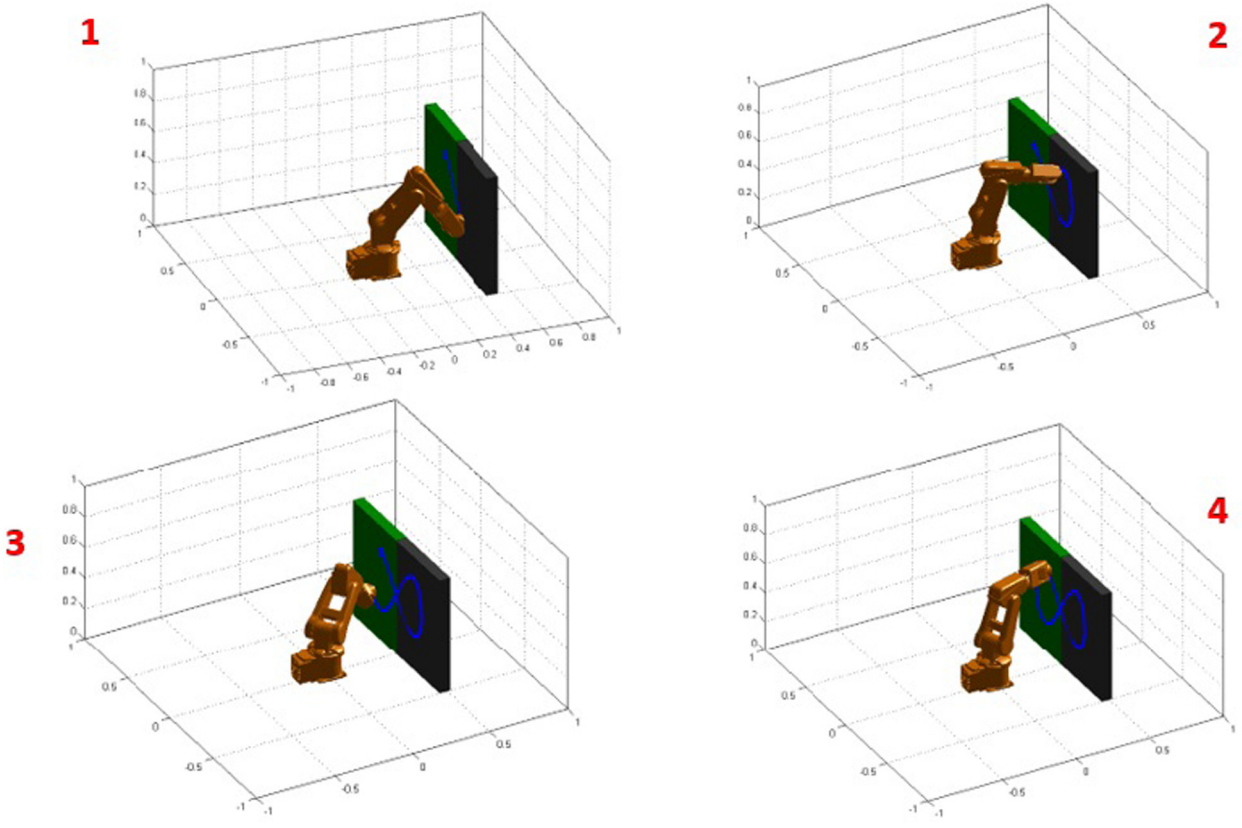

Fig. 13. Snapshots of the manipulator (IRB120) performing the task.

Please cite this article in press as: M.H. Hamedani et al., Recurrent fuzzy wavelet neural network variable impedance control of robotic manipulators with fuzzy gain dynamic surface in an unknown varied environment, Fuzzy Sets Syst. (2020), https://doi.org/10.1016/j.fss.2020.05.001

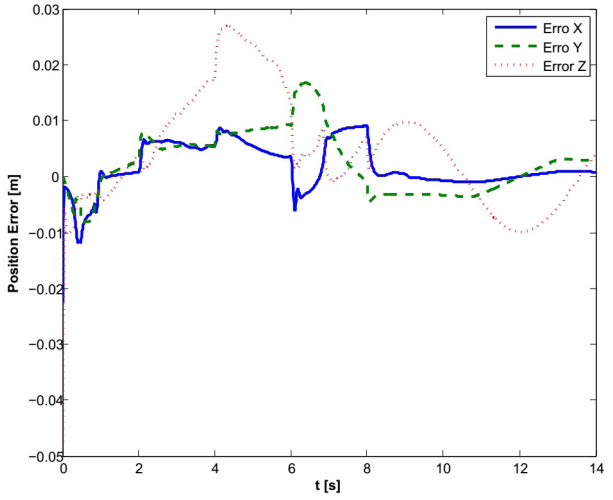

Fig. 14. Error Position tracking for proposed fuzzy gain dynamic surface (Case 1.2).

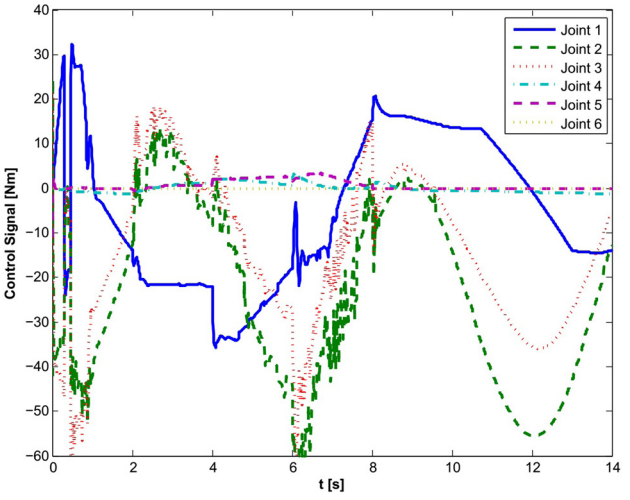

Fig. 15. Torque control signal for the proposed fuzzy gain dynamic surface (Case 1.2).

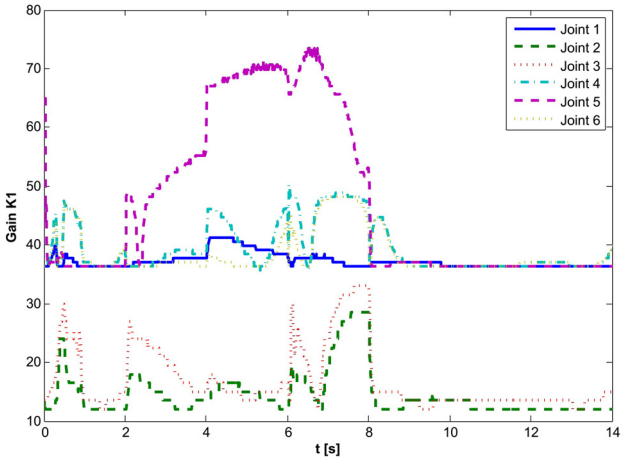

Fig. 16. Fuzzy Gain $\boldsymbol{K}_1$ each of the joints and for proposed fuzzy gain dynamic surface (Case 1.2).

Please cite this article in press as: M.H. Hamedani et al., Recurrent fuzzy wavelet neural network variable impedance control of robotic manipulators with fuzzy gain dynamic surface in an unknown varied environment, Fuzzy Sets Syst. (2020), https://doi.org/10.1016/j.fss.2020.05.001

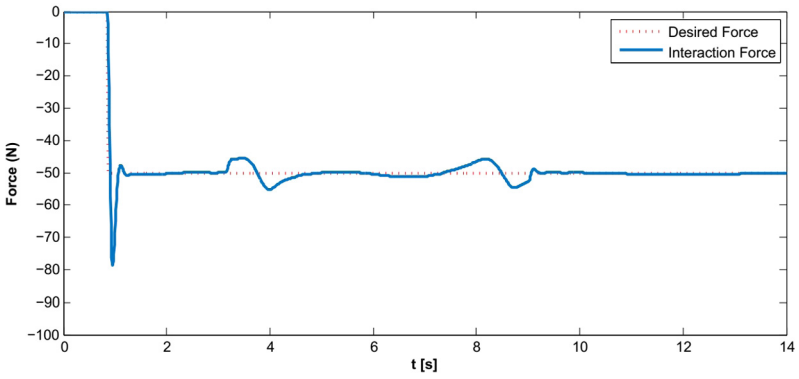

Fig. 17. Force tracking for General Impedance Profile (case 2).

Table 6
RMS of the signals of the Cases 1 and 2.

Signal / Method	Position Error X(m) (RMS)	Position Error Y(m) (RMS)	Position Error Z(m) (RMS)	Initial Contact Force (N)
General Impedance (Case 2)	0.0021	0.0031	0.0068	-78.6 N
Fuzzy Impedance (Case 2)	0.0021	0.0031	0.0068	-87.1
Proposed Intelligent Impedance (Case 2)	0.0019	0.0031	0.0068	-61.4

4.2. Case 2: intelligent impedance control

To consider the effect of the varied environment and evaluate the intelligent impedance control, three scenarios are introduced. In the first scenario, the general impedance profile is evaluated and drawbacks of the constant impedance parameters are discussed. In the second scenario, the intelligent impedance is proposed to improve the force tracking and to reduce the force contact. In the last scenario and in order to compare the proposed intelligent impedance to the other variable impedance, the fuzzy approach introduced in [7] is considered. It is worth noting that the gains of the dynamic surface are considered as case 1.2 without disturbance effect in (77). The constant parameters of the impedance profile are considered in (75). To establish a fair comparison, the controller parameters for the fuzzy impedance approach are chosen as $m_m = 2$, $d_s = 50$, $d_{med} = 150$, $d_b = 300$, $\lambda = 1/6$ and $k_p = k_n = 1$. In addition, for the intelligent impedance, the parameters of RFWNN are chosen as $\mu_v = 1000$, $\mu_f = 0.01$, $\gamma_1 = 0.7$, $\gamma_2 = 0.0001$ and $\mu = 0.6$. According to Eq. (53), we consider $k_s = 1$ for the simulation. In Fig. 3, the input vector is $x = [\tilde{x}, \dot{\tilde{x}}, \boldsymbol{e}_f]^T$ and five fuzzy rules and five wavelones are employed for RFWNN. From Fig. 17 and force tracking with constant impedance parameters, it can be observed that the performance of the robot is not acceptable because of the weak tracking and considerable error particularly at the initial contact $(-78.6N)$. In Fig. 18, the force tracking for fuzzy approach is depicted. It can be observed that force error during $3-9sec$ is decreased but the initial contact error is too large $(-87.1N)$. According to Fig. 19 and as a practical implementation point of view, the proposed adaptive algorithm effectively decreases the force error at the initial contact $(-61.4N)$ and the considerable constant error during $3-9sec$. As can be observed in Fig. 19, the transient response of force tracking is improved by using the proposed intelligent impedance in comparison with the general impedance in Fig. 17 and fuzzy impedance in Fig. 18. The proposed adaptive impedance controller is able to track the desired force and improve the interaction of the robot manipulator with the varied environment. According to Fig. 20, the parameters of RFWNN are online updated such that the impedance behavior of the system leads to promote the interaction of the robot with respect to environmental conditions and to effectively decrease the contact force error with an acceptable transient response. Accordingly, when the robot works on the varied environment, the impedance parameters (9) are adapted to track the desired force.

Table 6 provides the root mean square (RMS) of the position error and initial force error signal of case 2. This reveals that the proposed method improves the performance of the system by decreasing the position errors (RMS) and the magnitude of the initial force error signal (RMS).

Please cite this article in press as: M.H. Hamedani et al., Recurrent fuzzy wavelet neural network variable impedance control of robotic manipulators with fuzzy gain dynamic surface in an unknown varied environment, Fuzzy Sets Syst. (2020), https://doi.org/10.1016/j.fss.2020.05.001

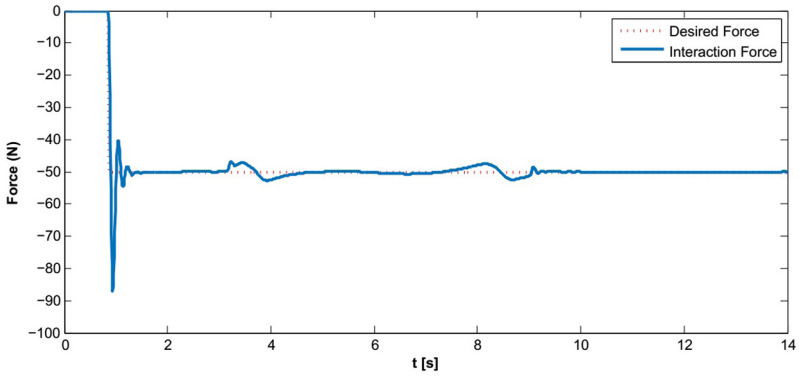

Fig. 18. Force tracking for fuzzy impedance approach (case 2).

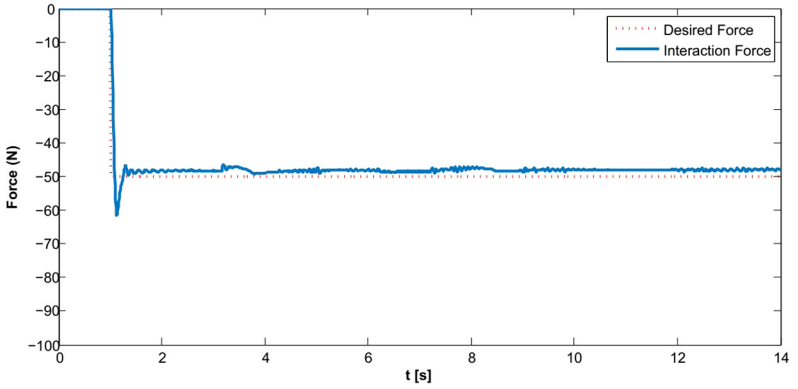

Fig. 19. Force tracking for proposed intelligent impedance approach (case 2).

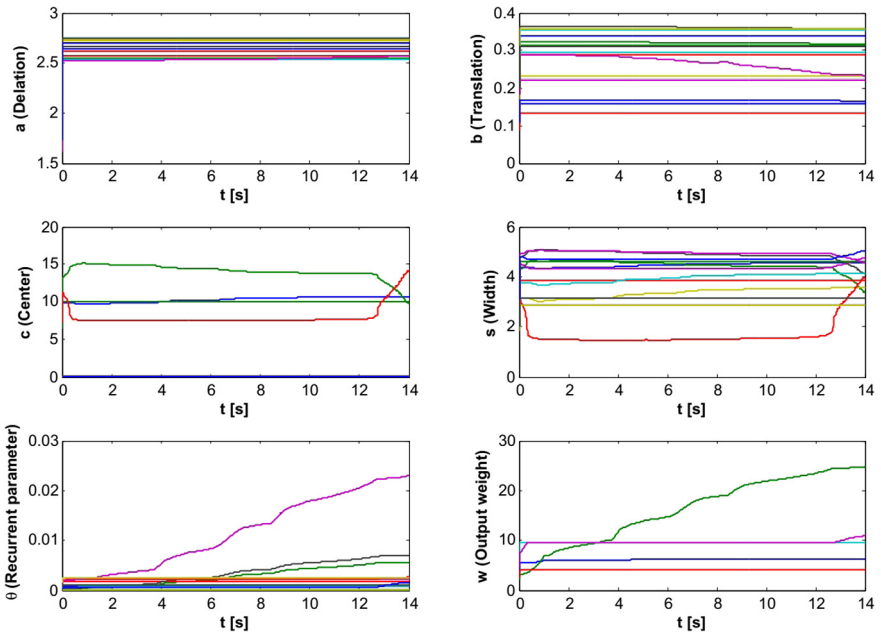

Fig. 20. Online updating of RFWNN parameters for intelligent impedance control (Case 2).

Please cite this article in press as: M.H. Hamedani et al., Recurrent fuzzy wavelet neural network variable impedance control of robotic manipulators with fuzzy gain dynamic surface in an unknown varied environment, Fuzzy Sets Syst. (2020), https://doi.org/10.1016/j.fss.2020.05.001

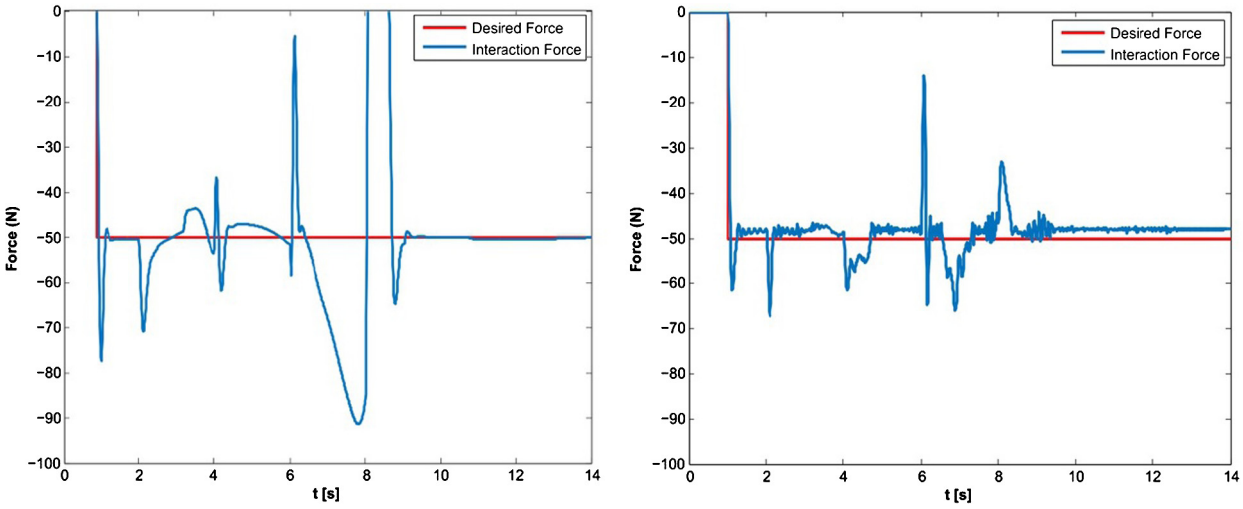

Fig. 21. Force tracking by considering the large disturbance effect for General Impedance Profile and constant gain dynamic surface (Left). Proposed Intelligent Impedance and fuzzy gain dynamic surface (Right) (case 2).

In the following case 2, we consider the proposed controller in the presence of disturbance (77). Fig. 21 shows that the combination of intelligent impedance and the fuzzy gain dynamic surface method is able to interact with unknown varied environment while the non-adaptive impedance profile and constant gain dynamic surface have large errors in force tracking and the manipulator leaves the wall during $8 - -9sec$; therefore, the interaction between the robot and environment is lost.

In this simulation, we consider two cases. In the first case, we evaluate the performance of the proposed fuzzy gain dynamic surface to reject the large and nonlinear disturbances when the control signals are bounded and position tracking is acceptable. Furthermore, the proposed intelligent impedance is able to adapt the parameters of RFWNN in order to improve the desired force tracking with respect to the unknown varied environment.

5. Conclusion

In this article, we have considered the combination of the fuzzy gain dynamic surface and intelligent impedance for the robotic manipulators. Fuzzy gain dynamic surface is proposed to make a robust control system overcome disturbance effect when the control signals are bounded and position tracking is acceptable. The formulation of the target impedance using effective dynamic surfaces error provides a simple structure to track the desired impedance. Based on the fuzzy set rules, the gains of the defined dynamic surface are tuned to observe disturbances. Consequently, the closed-loop system is robust against the external disturbances. In addition, the proposed variable impedance generates the desired impedance profile to interact with an unknown varied environment. Using the proposed learning approach of RFWNN, the impedance parameters are online updated to specify the new impedance profile as a desired impedance of the end-effector. The conditions of the stability and uniformly ultimately bounded stability of the closed-loop system are guaranteed by using Lyapunov's direct method. In the simulation studies, our approach is illustrated and evaluated in comparison to fixed gain dynamic surface and general impedance approach. Additionally, the results verify that the proposed controller is able to track a variable impedance model and interact with the unknown environment with good performance while the desired tracking force is acceptable.

Declaration of competing interest

The authors declare that they have no known competing financial interests or personal relationships that could have appeared to influence the work reported in this paper.

Please cite this article in press as: M.H. Hamedani et al., Recurrent fuzzy wavelet neural network variable impedance control of robotic manipulators with fuzzy gain dynamic surface in an unknown varied environment, Fuzzy Sets Syst. (2020), https://doi.org/10.1016/j.fss.2020.05.001

References

[1] N. Hogan, Impedance control: an approach to manipulation: Part ii—implementation, J. Dyn. Syst. Meas. Control 107 (1) (1985) 8–16.
[2] J. Buchli, F. Stulp, E. Theodorou, S. Schaal, Learning variable impedance control, Int. J. Robot. Res. 30 (7) (2011) 820–833.
[3] N. Roy, P. Newman, S. Srinivasa, Tendon-driven variable impedance control using reinforcement learning, Robot.: Sci. Syst. VIII (2013) 369–376.
[4] Z. Du, W. Wang, Z. Yan, W. Dong, W. Wang, Variable admittance control based on fuzzy reinforcement learning for minimally invasive surgery manipulator, Sensors 17 (4) (2017) 844.
[5] A. Enoch, S. Vijayakumar, Rapid manufacture of novel variable impedance robots, J. Mech. Robot. 8 (1) (2016) 011003.
[6] Y. Pei, G. Obinata, Y. Kim, J. Lee, Adaptive impedance control with variable viscosity for motion and force tracking system, in: 2015 International Symposium on Micro-NanoMechatronics and Human Science (MHS), 2015, pp. 1–5.
[7] L. Huang, S.S. Ge, T.H. Lee, Fuzzy unidirectional force control of constrained robotic manipulators, Fuzzy Sets Syst. 134 (1) (2003) 135–146.
[8] F. Ficuciello, L. Villani, B. Siciliano, Variable impedance control of redundant manipulators for intuitive human–robot physical interaction, IEEE Trans. Robot. 31 (4) (2015) 850–863.
[9] S. Arimoto, H.-Y. Han, P.T.A. Nguyen, S. Kawamura, Iterative learning of impedance control from the viewpoint of passivity, Int. J. Robust Nonlinear Control 10 (8) (2000) 597–609.
[10] H. Seraji, R. Colbaugh, Force tracking in impedance control, Int. J. Robot. Res. 16 (1) (1997) 97–117.
[11] N. Hogan, On the stability of manipulators performing contact tasks, IEEE J. Robot. Autom. 4 (6) (1988) 677–686.
[12] J.E. Colgate, N. Hogan, Robust control of dynamically interacting systems, Int. J. Control 48 (1) (1988) 65–88.
[13] K. Kronander, A. Billard, Stability considerations for variable impedance control, IEEE Trans. Robot. 32 (5) (2016) 1298–1305.
[14] A. Ramaratnam, N. Jalili, A switched stiffness approach for structural vibration control: theory and real-time implementation, J. Sound Vib. 291 (1–2) (2006) 258–274.
[15] F. Ferraguti, C. Secchi, C. Fantuzzi, A tank-based approach to impedance control with variable stiffness, in: 2013 IEEE International Conference on Robotics and Automation, 2013, pp. 4948–4953.
[16] M. Selvaggio, G.A. Fontanelli, F. Ficuciello, L. Villani, B. Siciliano, Passive virtual fixtures adaptation in minimally invasive robotic surgery, IEEE Robot. Autom. Lett. 3 (4) (2018) 3129–3136.
[17] T. Tsuji, M. Terauchi, Y. Tanaka, Online learning of virtual impedance parameters in non-contact impedance control using neural networks, IEEE Trans. Syst. Man Cybern., Part B, Cybern. 34 (5) (2004) 2112–2118.
[18] R.H. Abiyev, O. Kaynak, Fuzzy wavelet neural networks for identification and control of dynamic plants—a novel structure and a comparative study, IEEE Trans. Ind. Electron. 55 (8) (2008) 3133–3140.
[19] C.-J. Lin, C.-C. Chin, Prediction and identification using wavelet-based recurrent fuzzy neural networks, IEEE Trans. Syst. Man Cybern., Part B, Cybern. 34 (5) (2004) 2144–2154.
[20] L. Sheng, G. Xiaojie, Z. Lanyong, Robust adaptive backstepping sliding mode control for six-phase permanent magnet synchronous motor using recurrent wavelet fuzzy neural network, IEEE Access 5 (2017) 14502–14515.
[21] S. Chan, B. Yao, W. Gao, M. Cheng, Robust impedance control of robot manipulators, Int. J. Robot. Autom. 6 (4) (1991) 220–227.
[22] C.C. de Wit, B. Siciliano, G. Bastin, Theory of Robot Control, 2012.
[23] J.H. Oh, J.S. Lee, Control of flexible joint robot system by backstepping design approach, Intell. Autom. Soft Comput. 5 (4) (1999) 267–278.
[24] S. Tong, Y. Li, Adaptive fuzzy output feedback tracking backstepping control of strict-feedback nonlinear systems with unknown dead zones, IEEE Trans. Fuzzy Syst. 20 (1) (2011) 168–180.
[25] Q. Zhou, W. Wang, H. Liang, M. Basin, B. Wang, Observer-based event-triggered fuzzy adaptive bipartite containment control of multi-agent systems with input quantization, IEEE Trans. Fuzzy Syst. (2019).
[26] S.H. Kang, M. Jin, P.H. Chang, A solution to the accuracy/robustness dilemma in impedance control, IEEE/ASME Trans. Mechatron. 14 (3) (2009) 282–294.
[27] M. Krstic, I. Kanellakopoulos, V. Petar, Nonlinear and Adaptive Control Design, 1995.
[28] W. He, Y. Dong, C. Sun, Adaptive neural impedance control of a robotic manipulator with input saturation, IEEE Trans. Syst. Man Cybern. Syst. 46 (3) (2015) 334–344.
[29] M.-B. Cheng, W.-C. Su, C.-C. Tsai, T. Nguyen, Intelligent tracking control of a dual-arm wheeled mobile manipulator with dynamic uncertainties, Int. J. Robust Nonlinear Control 23 (8) (2013) 839–857.
[30] Z. Liu, J. Liu, W. He, Dynamic modeling and vibration control for a nonlinear 3-dimensional flexible manipulator, Int. J. Robust Nonlinear Control 28 (13) (2018) 3927–3945.
[31] J. Huang, C. Wen, W. Wang, Z.-P. Jiang, Adaptive stabilization and tracking control of a nonholonomic mobile robot with input saturation and disturbance, Syst. Control Lett. 62 (3) (2013) 234–241.
[32] L. Zhang, H.-K. Lam, Y. Sun, H. Liang, Fault detection for fuzzy semi-Markov jump systems based on interval type-2 fuzzy approach, IEEE Trans. Fuzzy Syst. (2019).
[33] H. Liang, L. Zhang, Y. Sun, T. Huang, Containment control of semi-Markovian multiagent systems with switching topologies, IEEE Trans. Syst. Man Cybern. Syst. (2019) 1–11.
[34] D. Swaroop, J.K. Hedrick, P.P. Yip, J.C. Gerdes, Dynamic surface control for a class of nonlinear systems, IEEE Trans. Autom. Control 45 (10) (2000) 1893–1899.
[35] P.P. Yip, J.K. Hedrick, Adaptive dynamic surface control: a simplified algorithm for adaptive backstepping control of nonlinear systems, Int. J. Control 71 (5) (1998) 959–979.
[36] S.J. Yoo, J.B. Park, Y.H. Choi, Adaptive dynamic surface control of flexible-joint robots using self-recurrent wavelet neural networks, IEEE Trans. Syst. Man Cybern., Part B, Cybern. 36 (6) (2006) 1342–1355.

Please cite this article in press as: M.H. Hamedani et al., Recurrent fuzzy wavelet neural network variable impedance control of robotic manipulators with fuzzy gain dynamic surface in an unknown varied environment, Fuzzy Sets Syst. (2020), https://doi.org/10.1016/j.fss.2020.05.001

[37] D. Wang, J. Huang, Neural network-based adaptive dynamic surface control for a class of uncertain nonlinear systems in strict-feedback form, IEEE Trans. Neural Netw. 16 (1) (2005) 195–202.
[38] B. Xu, Z. Shi, C. Yang, F. Sun, Composite neural dynamic surface control of a class of uncertain nonlinear systems in strict-feedback form, IEEE Trans. Cybern. 44 (12) (2014) 2626–2634.
[39] M.H. Hamedani, M. Zekri, F. Sheikholeslam, Adaptive impedance control of uncertain robot manipulators with saturation effect based on dynamic surface technique and self-recurrent wavelet neural networks, Robotica 37 (1) (2019) 161–188.
[40] S.A.M. Dehghan, M. Danesh, F. Sheikholeslam, M. Zekri, Adaptive force–environment estimator for manipulators based on adaptive wavelet neural network, Appl. Soft Comput. 28 (2015) 527–540.
[41] Q. Zhang, A. Benveniste, Wavelet networks, IEEE Trans. Neural Netw. 3 (6) (1992) 889–898.
[42] J. Zhang, G.G. Walter, Y. Miao, W.N.W. Lee, Wavelet neural networks for function learning, IEEE Trans. Signal Process. 43 (6) (1995) 1485–1497.
[43] Y. Oussar, I. Rivals, L. Personnaz, G. Dreyfus, Training wavelet networks for nonlinear dynamic input–output modeling, Neurocomputing 20 (1–3) (1998) 173–188.
[44] B.R. Bakshi, G. Stephanopoulos, Wave-net: a multiresolution, hierarchical neural network with localized learning, AIChE J. 39 (1) (1993) 57–81.
[45] O. Rioul, M. Vetterli, Wavelets and signal processing, IEEE Signal Process. Mag. 8 (1991) 14–38.
[46] F.-J. Lin, H.-J. Shieh, P.-H. Shieh, P.-H. Shen, An adaptive recurrent-neural-network motion controller for xy table in cnc machine, IEEE Trans. Syst. Man Cybern., Part B, Cybern. 36 (2) (2006) 286–299.
[47] C.-M. Lin, C.-F. Hsu, Recurrent-neural-network-based adaptive-backstepping control for induction servomotors, IEEE Trans. Ind. Electron. 52 (6) (2005) 1677–1684.

Please cite this article in press as: M.H. Hamedani et al., Recurrent fuzzy wavelet neural network variable impedance control of robotic manipulators with fuzzy gain dynamic surface in an unknown varied environment, Fuzzy Sets Syst. (2020), https://doi.org/10.1016/j.fss.2020.05.001